

## Chapter 3

# FAULT EVENTS CLASSIFICATION USING DWT & MACHINE LEARNING TECHNIQUES

---

### 3.1 Introduction

The transmission networks are integral segment of the power system. These are widely dispersed over the country and usually suffers from different short-circuit events due to the sustained increase in electrical and environmental stress. The power outages caused due to fault events have a profound impact on the growth of any nation. Hence it is imperative to utilize intelligent protection mechanisms for the modern power grid, which are competent in providing faster restoration of the transmission network. In this chapter, the structure of the proposed integrated signal processing and machine learning based methodology for ascertaining the fault events in the compensated power transmission network is presented. The work-flow of the proposed fault ascertaining mechanism is shown in Figure 3.1. The principal idea is to identify the critical features in the post fault current samples by applying pertinent signal processing mechanism and apply those selected feature vectors to the machine learning based models as training and testing dataset for ascertaining the categories and location of the faults in the circuit. The designed classifier model predicts the type of fault events in the network as its output. In addition, the basics of machine learning algorithm, particularly non-parametric machine learning techniques are briefly described in this chapter. Further, the strength and workability of the proposed integrated DWT and non-parametric ML based fault events ascertaining methodology is analyzed for

various fault scenarios in two distinct simulated test networks. In the last section, a comparative analysis of the classification accuracy obtained by the proposed non-parametric classifier models during various test cases is summarized.

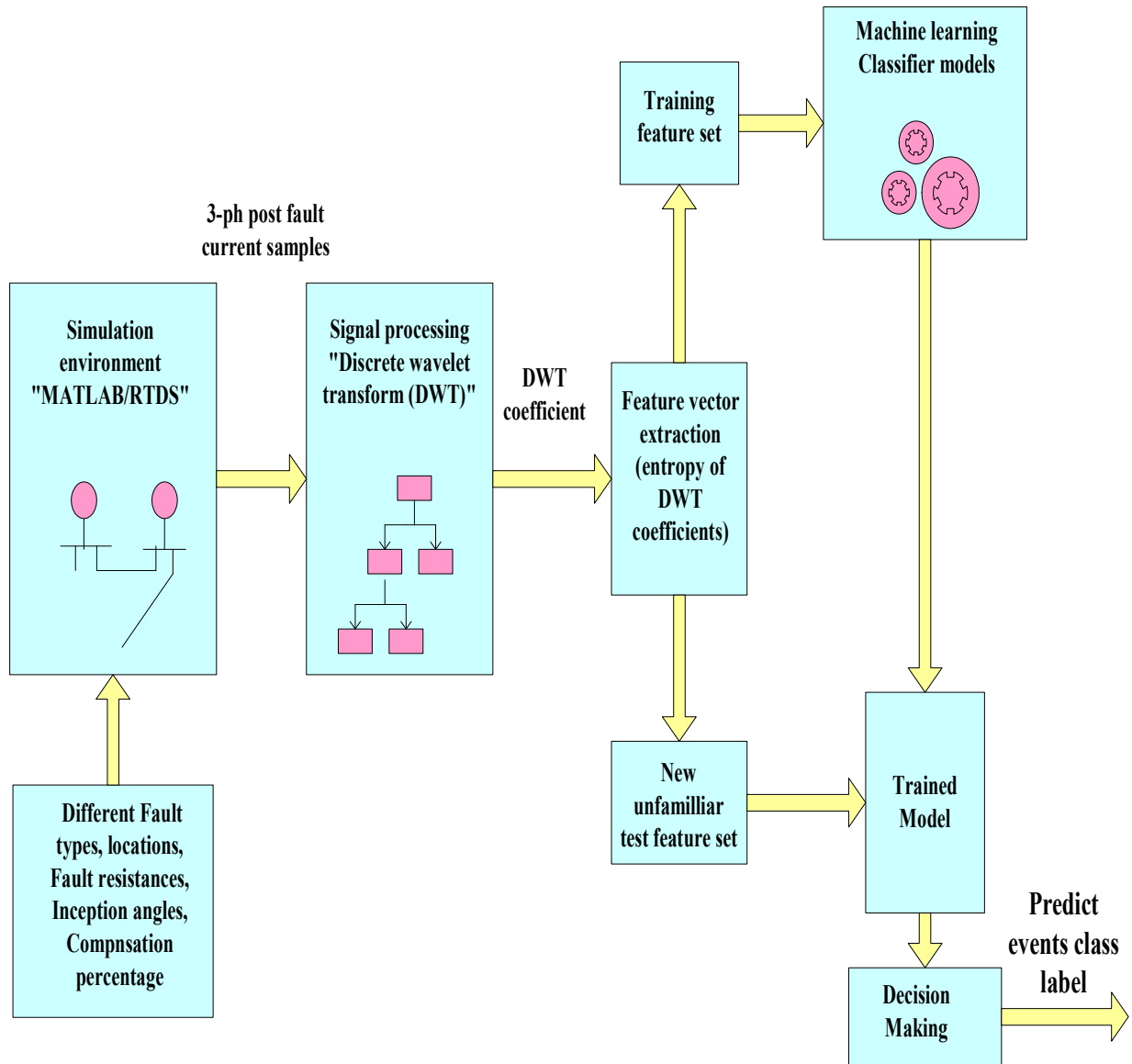


Figure 3.1 Work flow of the proposed events classification scheme

### 3.2 Machine Learning Techniques

In the past few decades, terms like intelligent computing, machine learning (ML), and deep learning are predominantly utilized in various applications in different fields such as engineering, bioinformatics, medicine, and financial markets. Utilization of these mechanisms comprehensively helps in rapid analysis and prediction of best outcome. Recently, ML based mechanism is very commonly applied in different applications like in identification of spam mails, face detection, disease diagnosis, in financial marketing, in accident prone vehicles. The term ML can be characterized as a set of methods based on computer science and statistical analysis that has the strength of recognizing the meaningful pattern of any samples by data mining and making the verdict about the unfamiliar data set [95-97]. According to Tom M. Mitchell it can be defined as “the collection of algorithms that improve their performance  $P$  with respect to task  $T$  with experience  $E$ ” [98]. It is simply the application of intelligent mechanism that helps the system to learn automatically by understanding the patterns of the training dataset and improve from experiences. The functioning of machine learning is represented in Figure. 3.2 [98]. For developing a machine learning based algorithm following steps are involved-

- i) Acquire the feature dataset
- ii) Pre-process/ Analyse the dataset
- iii) Train the algorithm with input dataset
- iv) Test the algorithm with unfamiliar dataset
- v) Predict the decision

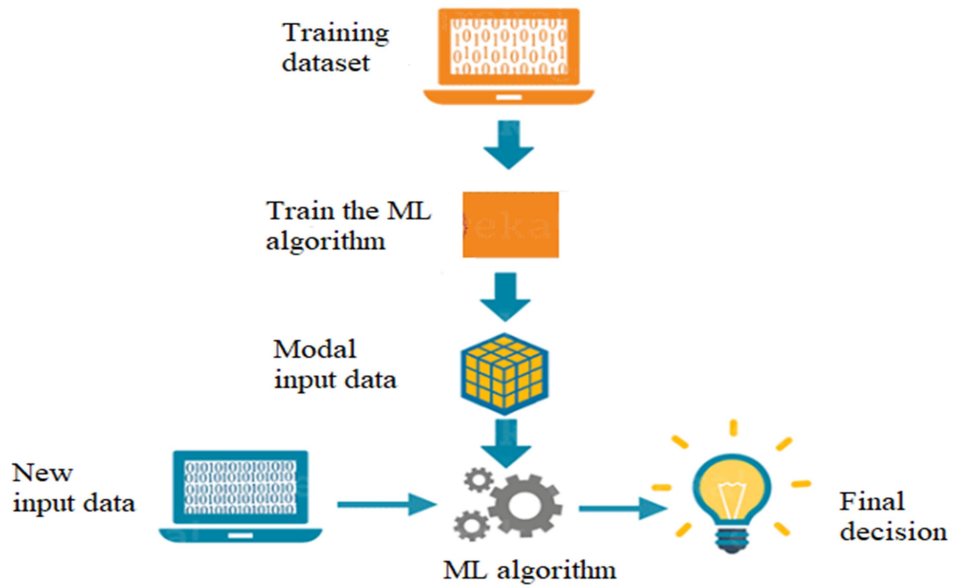


Figure 3.2 Functioning of Machine learning

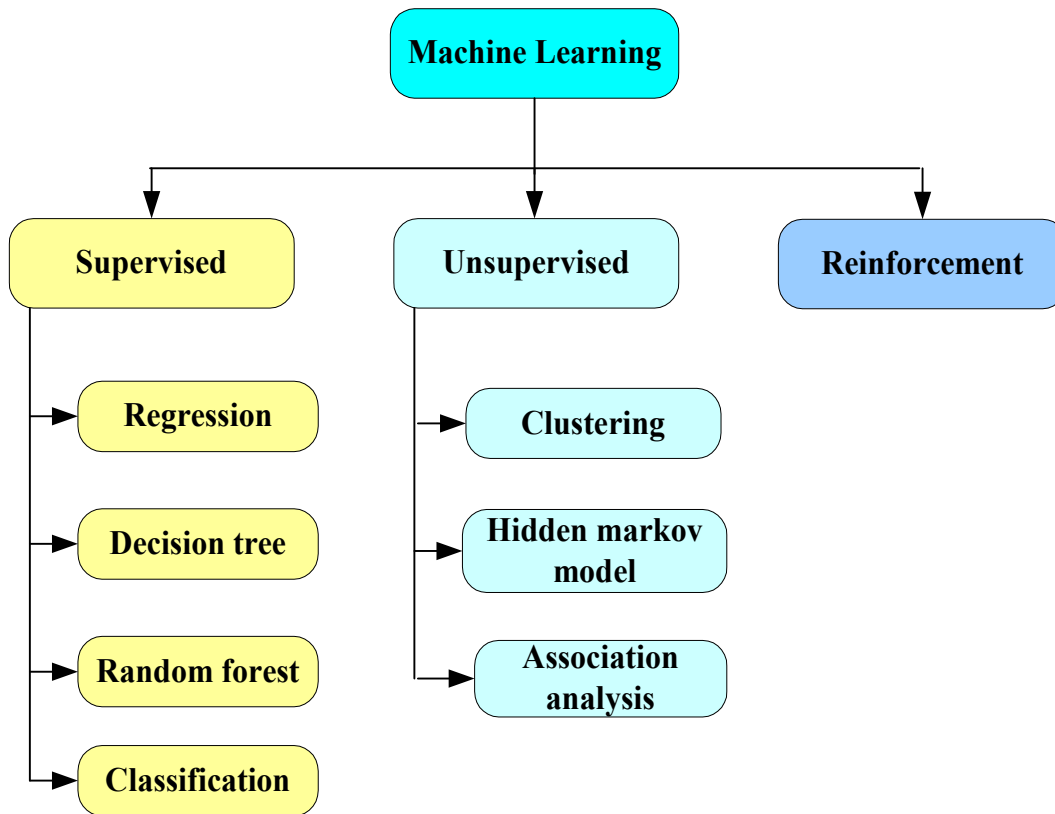


Figure 3.3 Classification of machine learning techniques

On the basis of adopted learning mechanism the ML algorithms can be categorized in following types [98] (as shown in Figure. 3.3)-

- i) Supervised learning
- ii) Un-supervised learning
- iii) Reinforcement learning

*Supervised learning:* In this learning strategy, the training dataset composed of respective features with corresponding target label. The model recognizes the pattern of the features corresponding to individual classes in the dataset that can be further utilized for making the verdict about the unfamiliar data set.

*Unsupervised learning:* In this learning strategy, no class label is provided in the training dataset. In contrast, the algorithm itself tries to identify the specific similarities in the input dataset so that the original dataset can be categorized into similar groups. Clustering and self-organizing mapping methods are most common examples of it.

*Reinforcement learning:* This learning scheme lies in between supervised and unsupervised learning strategy. The algorithm gets informed if the prediction is incorrect, but does not inform how to correct it. It has to search and make out different possibilities until it works out how to get the answer right. Sometimes it is also called learning with a critic because of this monitor that check the answer, but does not recommend the improvements.

### 3.2.1 Parametric Machine Learning Algorithms

The ML algorithms can also be classified as parametric and non-parametric algorithms. Figure 3.4 represents another categorization of machine learning computing techniques which are widely applied for classification and regression analysis [99]. A classifier model

which can be characterized by a confined number of parameters is called as parametric model whereas, those models which cannot be parameterized by a finite number of parameters set are termed as the non-parametric model [99]. In a parametric ML model, each of the training features have its influence on the final decision estimation, whereas in the nonparametric algorithms, there is no single global mechanism; local models are computed as they are needed, influenced only by the nearby training feature sets. In a parametric approach, the model is straightforward, simple and has a small number of parameters.

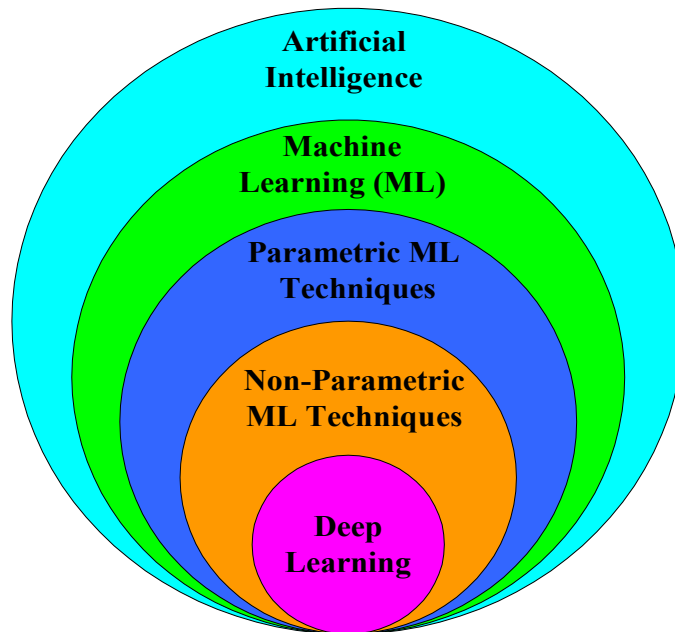


Figure 3.4 Categories of Machine learning algorithms

Types of Parametric Machine learning Algorithms are as follows:

- i) Naïve Bayes (NB)
- ii) Linear regression
- iii) Linear discriminant analysis (LDA)
- iv) Quadratic discriminant analysis (QDA)

### 3.2.2 *Non-Parametric Machine Learning Algorithms*

The ML algorithms which do not considered any presumptions regarding the form of the mapping function are termed as non-parametric ML Algorithms. These algorithms are also called as instance-based or memory-based learning algorithms, since what they do is to accumulate the training feature sets in a lookup table and interpolate from those. It also refers as lazy learning mechanism as it do not estimate the model when the training set is provided just like parametric algorithms, it delayed the computation of the model till the testing instances are provided. The types of Non-Parametric machine learning algorithms are:

- i) K-nearest neighbor (K-NN)
- ii) Support Vector machine with Gaussian kernels
- iii) Probabilistic Neural Network

### 3.3 **K-Nearest Neighbor (K-NN) Technique**

K-NN has been efficiently used in various applications like pattern recognition, image processing, and text classification. The principle behind the prediction of the class of new instance (test samples) using K-NN algorithm is to compute its distance from all training samples. The particular class assigned on the basis of majority votes of its neighbors, from which it has the least distance [100-101]. In the present designed K-NN based classifier model, exhaustive search method is applied for computing the distance of test sample from trained samples. It ranks the computed distance in ascending order according to lowest distances. Apart of various distance metrics (Euclidean, Minkowski, Mahalanobis etc) in

K-NN, Minkowski metric has been applied for computing the distance, as given in equation (7). Smallest break-ties index has been used for cases if multiple classes have the same smallest distance. Once the k-nearest neighbors of a test sample are obtained, distance weight functions are used for evaluating them. The main objective of weight function is to remove the effect of distant neighbors on the majority vote. Inverse distance weight function is used in this work. The algorithm of the applied K-NN technique is given below and the details of the used parameters of K-NN are listed in the Appendix.

$$D_{(x,y)} = p \sqrt[p]{\sum_{i=1}^n |x_i - y_i|^p} \quad (3.1)$$

---

#### Algorithm K-Nearest Neighbour

---

##### 1. Training phase:

- Initialization of feature vectors as training data set
- define the number of nearest neighbors (positive integer)
- define NS-Method 'exhaustive'
- define Distance-Weight 'inverse' and Distance-function 'minkowski'
- define break-ties
- Store the feature vectors with associated class labels

##### 2. Classification phase:

- The test cases are classified on basis of majority vote of its neighbors.
    - Compute its distance from trained samples using Distance-function 'minkowski'.
    - The particular class of test case is ascertained on the basis of majority votes of its neighbors, from which it has least distance.
-



### 3.4 Support Vector Machine (SVM) Technique

SVM technique has been commonly been used in multiple analysis of the power system due to its high competency in handling large feature data set and less chance of getting local convergence. It endeavors a hyper plane for segregating the data points according to their specific class label [102]. When the separations between the specific class labels are optimal, then the corresponding plane is called as optimal hyper-plane. Principally it is a binary classification technique; however, it can be utilized for multi-class categorization using one Vs all algorithm. In present work, SVM has been applied for discriminating 10 different kinds of fault events in the compensated power network, hence one vs all mechanism has been utilized. The quadratic Gaussian function is used as the kernel function. The sequential minimal optimization method is utilized for the separation of the hyper-plane. The principle behind SVM mechanism is explained below by taking an example of binary classification. Let the two classes dataset are built of n data samples.

$$\{E_i, F_i\}_{i=1}^n \quad (3.2)$$

$$W^T E_i + b = 0 \quad (3.3)$$

$E_i \in$  Entropy value and  $F_i \in \{-1,1\}$  i.e. corresponding fault class label. Binary classification using SVM mechanism is shown in Figure 3.5. The equation (3.3) is the expected hyper-plane which recognizes the dataset into its associated class label. W is associated weight vector. It has been computed keeping the separation in class labels optimal. Separation margin  $S_m$  is given by-

$$S_m = \frac{2}{\|W\|} \quad (3.4)$$

For maximum  $S_m$ ,  $\|W\|$  should be minimum. Therefore, the needed SVM can be formulated by minimizing  $\nu(W)$  expression given below

$$\nu(W) = \frac{1}{2} W^T W$$

Subjected to constraint  $F_i(W^T E_i + b) \geq 1$

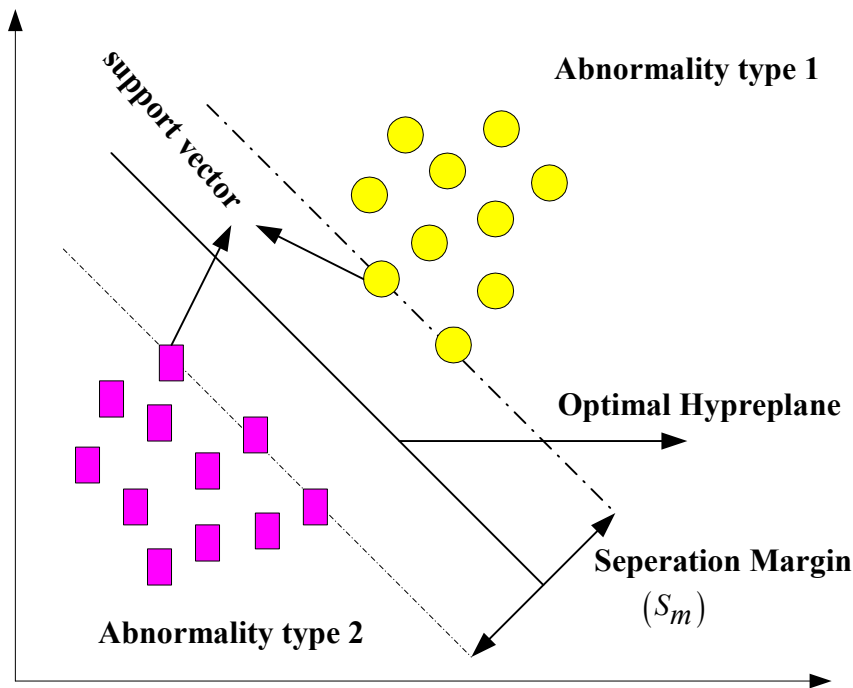


Figure 3.5 Two class separation using SVM

### 3.5 Probabilistic Neural Network (PNN)

PNN technique has been usually utilized in different classification applications, mainly due to its patterns mapping capability. It simply involves estimation of probability density function (PDF) of feature samples of each class. The classification of the events class labels has been accomplished by utilizing the computed PDF in accordance with Baye's rules.

The PNN model is comprised of an input layer, two hidden layers (namely pattern and summation) and output layers, organized in a successive sequence as shown in Figure. 3.6.

Once the  $e_a$ ,  $e_b$ ,  $e_c$  values, i.e. the realized feature set of 3-phases have been fed to the pattern layer from the input layer, the neuron's estimated its closeness from the trained feature set, by using expression given below:

$$f_{A(x)} = \frac{1}{(2\pi)^{k/2} \sigma^k} \exp \left[ -\frac{(x-x_{Ai})^T (x-x_{Ai})}{2\sigma^2} \right] \quad (3.5)$$

Where,  $\sigma$  is the smoothing parameter;  $k$  is the dimension. Thereupon the summation layer added up all the inputs received by pattern layer for each class and produces a net output of probability. Finally, the Baye's decision rule has been utilized for deciding the associated class label of the test event samples once the summation of weighted votes for each category has been computed. The class with largest vote probability is said to be the particular category of the test sample.

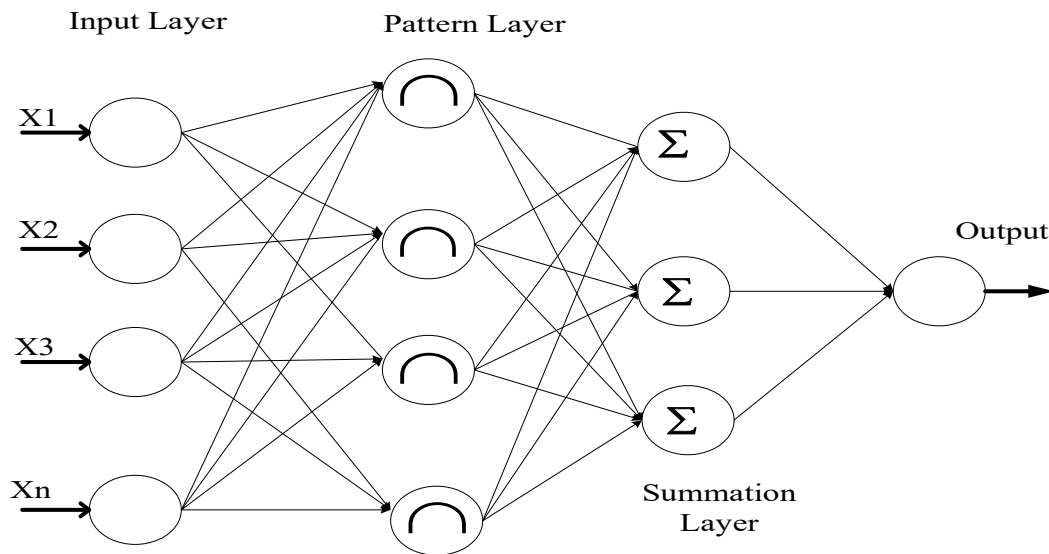


Figure 3.6 Architecture of PNN

### 3.6 Proposed DWT and Non-Parametric ML based Fault Events Classification Scheme

The flow chart of the proposed integrated DWT and non-parametric ML based fault events classification scheme is shown in Figure 3.7. The prime idea is to pick the dominant features of the fault current signal and to apply it to the parametric ML classifier models for categorizing the fault events in the transmission system. First of all, the retrieved 3-phase post fault current samples are segmented into different levels using Db5 mother wavelet. Consequently, the effective fault signatures have been extracted as the feature vectors in terms of norm entropy of the DWT coefficients ( $e_a$ ,  $e_b$ , and  $e_c$ ) as explained in section 2.6. Thereafter, the computed entropy of each phase is applied as input to the non-parametric ML classifier models as training and testing dataset. During the training phase, the classifier models recognise the pattern of the feature vectors associated with different kinds of shunt fault events in the transmission circuit. Further, in the testing phase feature sets of new unfamiliar fault cases with varying circumstances are applied to the trained classifier model and the model predicts the particular category of the test instance as its final output. The detail training mechanism of the non-parametric ML classifier model and considered test cases are thoroughly discussed in the next section.

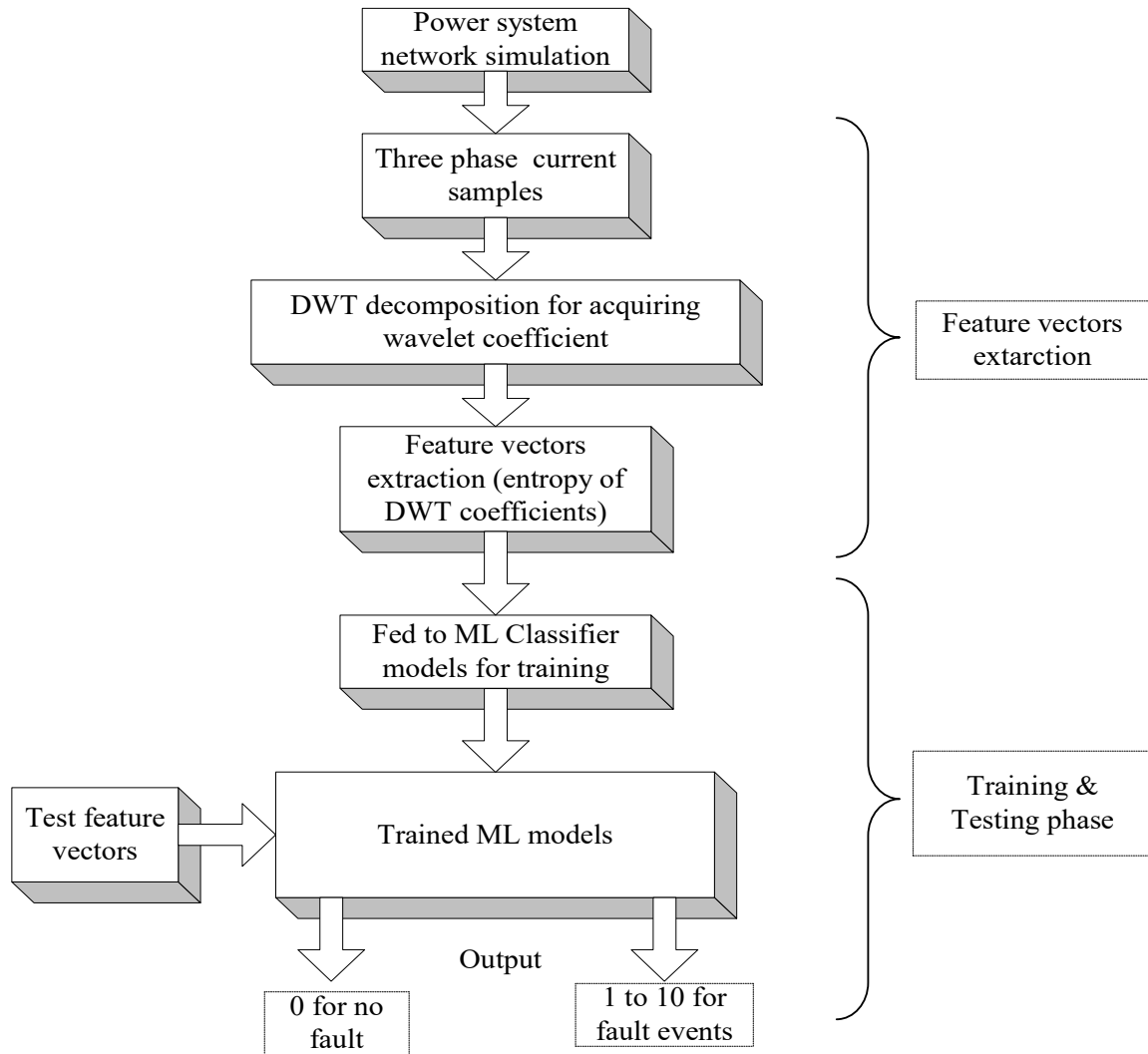


Figure 3.7 Flow-chart of the proposed fault events classification scheme

### 3.6.1 Training and Testing Mechanism

In the present work, three different non-parametric ML classifier models (K-NN, SVM, and PNN) are utilized for ascertaining the distinctive fault categories in the compensated power transmission networks. In the training phase the computed feature vectors in terms of entropy of DWT coefficients ( $e_a$ ,  $e_b$ , and  $e_c$ ) corresponding to various scenarios such as normal operating mode and during abnormal fault events (with varying conditions like fault

types, location of faults, fault resistances, inception angles and percentage of line compensation) are fed as input dataset to the non-parametric ML classifier models. Various fault scenarios in the transmission network are labelled as follows: class 0 (no fault), class 1 (a-g), class 2 (b-g), class 3 (c-g), class 4 (a-b), class 5 (a-c), class 6 (c-b), class 7 (abg), class 8 (bcg), class 9 (acg), class 10 (abc). The details of various considered training and testing conditions on the first test network are depicted in Table 3.1. The test sample are consists of feature vectors corresponding to 10 normal operating modes and various fault conditions including 7 different new locations in the network, six fault resistances, six fault inception angles, and two level of line compensation percentage. Hence, the total size of the testing samples is 5050 (10 samples of normal operation and 5040 samples of fault cases). The classifier model identifies the pattern of the feature vectors associated with different fault scenarios in the transmission network using its computing algorithms. After the training period, the classifier models can predict the category of the unknown test instance based on the identified training pattern set. Further, during the competency assessment of the proposed events classification scheme, the features vectors corresponding to different considered test cases have been applied to the trained ML classifier model as input, and the classifier model predicts the particular category of the events in the network as its output from 0 to 10 labels.

**Table 3.1** Training and testing conditions considered on first test system

S. No	Parameters	Training cases	Testing cases
1.	Fault locations	Twenty different locations	Seven new unknown location (30 km, 50km, 110 km, 170 km, 190 km, 230 km and 250 km)
2.	Fault Resistance (ohms)	0.001, 20, 60	0.1, 0.5, 1, 5, 10, 50
3.	Fault inception angle (°)	0, 75, 150	30, 45, 60, 90, 120, 135
4.	Fault events types	No fault and all kinds faults events	Unknown no fault and all kinds of fault events
5.	Level of line compensation	35 % and 45 %	30 % and 40 %

### 3.7 Case Study and Results

The proposed DWT and non-parametric ML based fault events categorization scheme has been extensively tested for various cases (such as normal operating mode, different kinds of fault events, with varying system conditions like fault resistance, fault inception angles, locations in the transmission network, and level of line compensation percentage) for evaluating its competency and feasibility in diagnosing the fault events in compensated power network (in MATLAB environment). Three different non-parametric ML classifier models are utilized in this work for ascertaining the fault events in the transmission network. The classifier models give its output from 0 to 10 during the testing phase. The zero output declares the normal operating mode of the power network without any abnormality, while if the output of the models lies between 1 to 10 it indicates that particular type of fault occurred in the network.

### 3.7.1 Test Case I: Two-Bus Series Compensated Transmission Test Network

A long mid-point capacitor compensated transmission system (300 km) with 400 kV, 50 Hz is simulated in the MATLAB (as shown in Figure 3.8) for evaluating the efficaciousness of the proposed fault events ascertaining scheme. The designed network details (like line parameters and compensation ratings) are listed in appendix. Four levels of capacitor compensation percentage i.e. 30 %, 35 %, 40 % and 45 % have been applied at the central position of the transmission network. The CT with 2000:5 A has been utilized for acquiring the post fault current samples. The sampling frequency used is 20 kHz. The ratings of the MOV utilized for guarding the compensating capacitor elements is fixed 2.5 times times that of nominal capacitor voltage. The single side current measurement is utilized in the present work. The 3-phase post fault current samples for various fault scenarios have been utilized for performing the fault analysis. All sorts of shunt fault events with varying conditions such as fault resistance, inception angles, location of events, and different percentage of line compensation have been considered during the testing. Along with the usual inter-circuit fault events, evolving abnormality cases are also simulated in the test network. The efficacy and feasibility of the proposed events ascertaining scheme has also been evaluated for transforming fault cases in the compensated transmission system. Figure 3.9 represents the 3-phase post fault (A-G) current samples with respect to time (s) at 30 km from the sending side on different inception angle. The 3-phase post fault current samples measured from the sending side are segmented in different levels using Db5 mother wavelet. Subsequently, the effective fault feature vectors are extracted in terms of norm entropy of the DWT coefficients of each phase. Then the computed feature vectors corresponding to different abnormality scenarios are fed as input to the non-parametric ML



classifier models. Eventually, the classifier model predicts the corresponding class of the test instance on the basis of trained pattern set as its output. The fault events classification accuracy of the proposed events categorization strategy is computed by equation-(3.6).

$$Classification_{accuracy}(\%) = \frac{(\text{Total correct classified events})}{\text{Total number of test events}} \times 100 \quad (3.6)$$

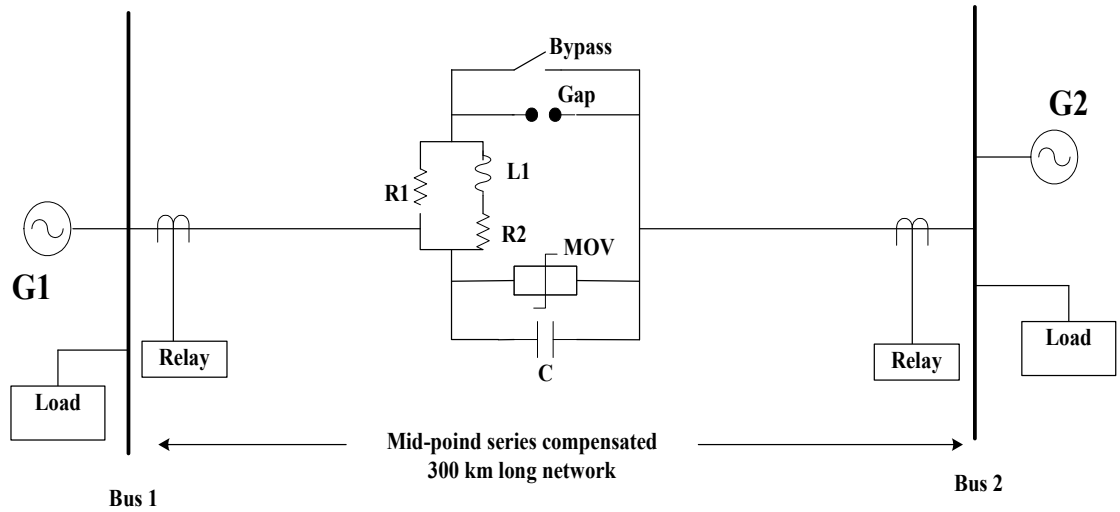
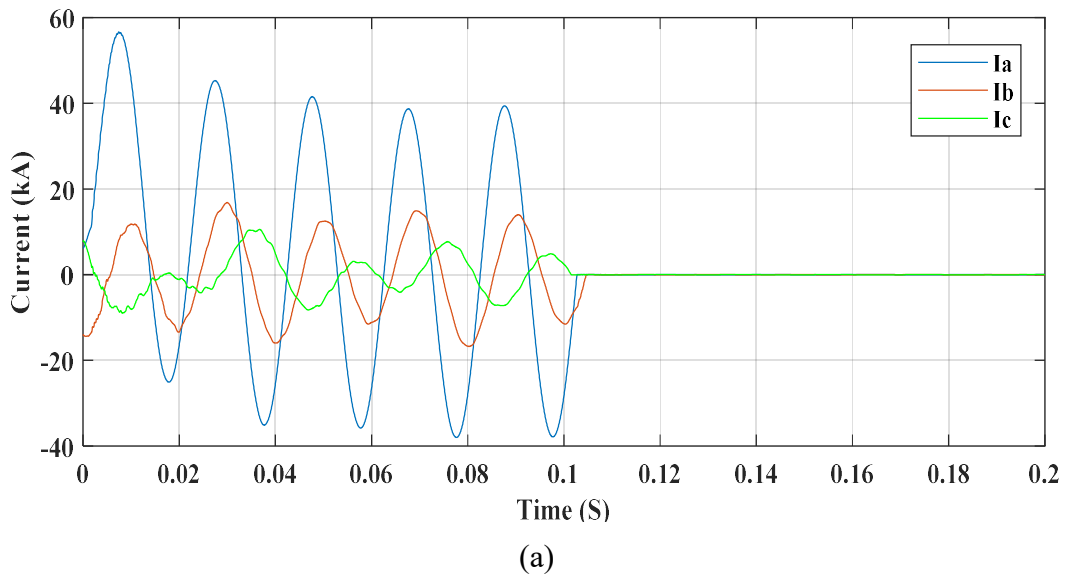
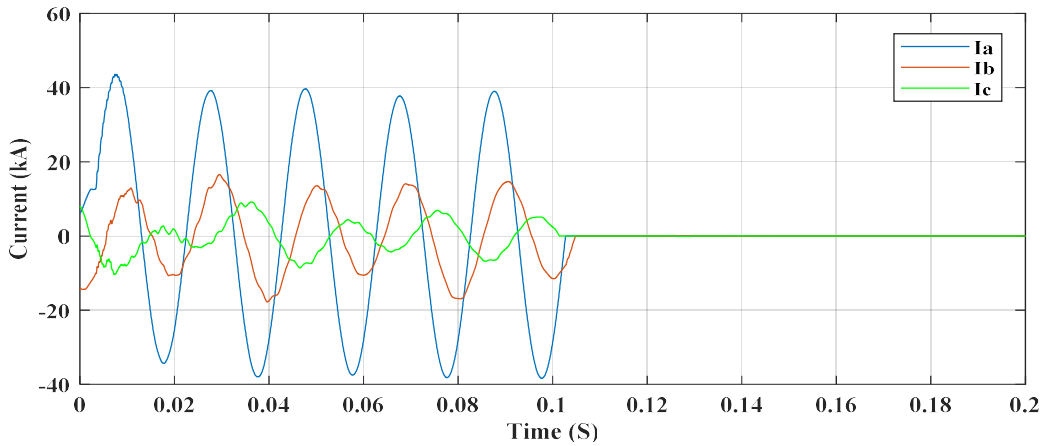
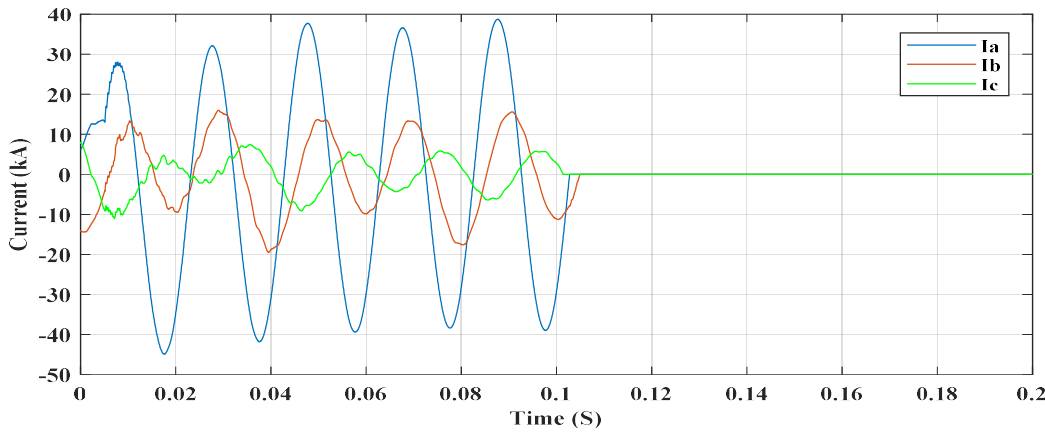


Figure 3.8 Two-bus mid-point compensated network (first test system)

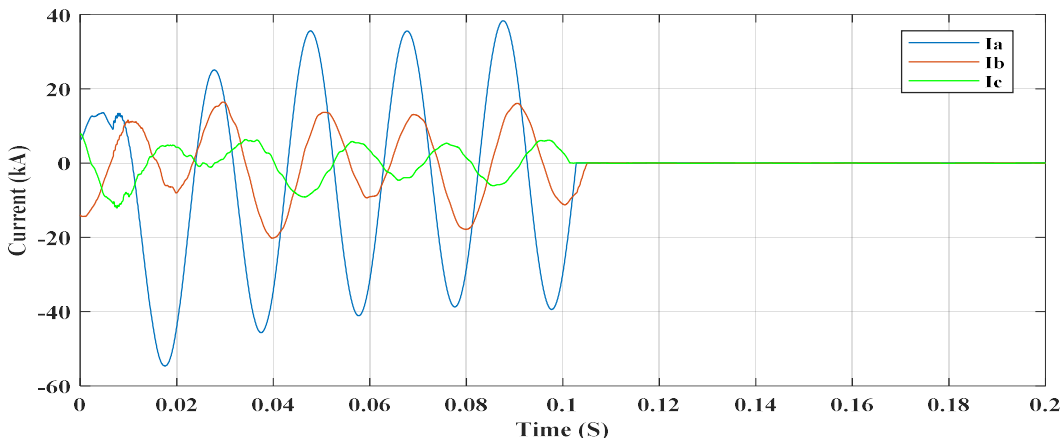




(b)



(c)



(d)

Figure 3.9 Three phase current signals during line to ground fault event at 30 km on different inception angles (a) 30 degree; (b) 60 degree; (c) 90 degree; (d) 120 degree

Table 3.2 shows the fault events classification accuracy percentage acquired by the proposed DWT and K-NN based scheme during various considered test cases. From Table 3.2, it can be observed that proposed K-NN based scheme gives 100% classification accuracy for most common fault (LG) and extremely severe fault (LLL) events. Similarly, the classification accuracy achieved for LL and LLG fault events are 99.140% and 98.478% respectively. The overall average fault events classification accuracy obtained by the proposed K-NN classifier model based scheme is 99.404%. In addition, Table 3.3 shows the variation of obtained classification accuracy with respect to the number of nearest neighbor ‘K’ selected. Table 3.4 shows the corresponding confusion matrix obtained during testing of K-NN based scheme.

**Table 3.2** Faults classification accuracy percentage obtained by K-NN technique based scheme

Fault type	Number of test samples	Number of incorrect classification	Correct classification	Over all Accuracy (%)
Line to Ground	1512	0	1512	100.00
Line to Line	1512	13	1499	99.140
Double Line to Ground	1512	23	1489	98.478
3 phase (LLL)	504	0	504	100.00
Avg. Accuracy				<b>99.404</b>

**Table 3.3** Variation of obtained accuracy percentage with respect to change in ‘K’ values

S. No.	Fault events type	K-NN Classifier Model Accuracy (%)		
		K=1	K=3	K=5
(i)	Line to Ground	100.00	100.00	100.00
(ii)	Line to Line	99.404	100.00	98.809
(iii)	Double Line to Ground	98.214	97.619	99.404
(iv)	3 phase (LLL)	100.00	100.00	100.00
(v)	Avg. Accuracy	<b>99.404</b>	<b>99.404</b>	<b>99.553</b>

**Table 3.4** Confusion matrix for the KNN based scheme (First test system)

Actual fault events	Sample size	Predicted fault events											Accuracy (%)
		AG	BG	CG	AB	AC	BC	ABG	BCG	ACG	ABC	No fault	
AG	<b>504</b>	<b>504</b>	0	0	0	0	0	0	0	0	0	0	<b>100</b>
BG	<b>504</b>	0	<b>504</b>	0	0	0	0	0	0	0	0	0	<b>100</b>
CG	<b>504</b>	0	0	<b>504</b>	0	0	0	0	0	0	0	0	<b>100</b>
AB	<b>504</b>	0	0	0	<b>500</b>	0	0	<b>4</b>	0	0	0	0	<b>99.2</b>
AC	<b>504</b>	0	0	0	0	<b>498</b>	0	0	0	<b>6</b>	0	0	<b>98.8</b>
BC	<b>504</b>	0	0	0	0	0	<b>501</b>	0	<b>3</b>	0	0	0	<b>99.4</b>
ABG	<b>504</b>	0	0	0	<b>8</b>	0	0	<b>496</b>	0	0	0	0	<b>98.4</b>
BCG	<b>504</b>	0	0	0	0	0	<b>3</b>	0	<b>501</b>	0	0	0	<b>99.4</b>
ACG	<b>504</b>	0	0	0	0	<b>12</b>	0	0	0	<b>492</b>	0	0	<b>97.6</b>
ABC	<b>504</b>	0	0	0	0	0	0	0	0	0	<b>504</b>	0	<b>100</b>
No fault	<b>10</b>	0	0	0	0	0	0	0	0	0	0	<b>10</b>	<b>100</b>

Table 3.5 provides the fault events classification accuracy percentage obtained by the DWT and SVM based scheme during testing. It has been seen that proposed SVM based scheme also gives 100% classification accuracy for LG and LLL fault events. However, the classification accuracy achieved for LL and LLG fault events are 98.61% and 98.94% respectively. The overall average fault events classification accuracy obtained by the proposed SVM based scheme is 99.39%. Table 3.6 shows the corresponding confusion matrix obtained during testing of SVM based scheme.

**Table 3.5** Faults classification accuracy percentage obtained by SVM technique based scheme

Fault type	Number of test samples	Number of incorrect classification	Correct classification	Over all Accuracy (%)
Line to Ground	1512	0	1512	100.00
Line to Line	1512	21	1491	98.61
Double Line to Ground	1512	16	1496	98.94
3 phase (LLL)	504	0	504	100.00
Avg. Accuracy				<b>99.39</b>

**Table 3.6** Confusion matrix for the SVM based scheme (First test system)

Actual fault events	Sample size	Predicted fault events											Accuracy (%)
		AG	BG	CG	AB	AC	BC	ABG	BCG	ACG	ABC	No fault	
AG	504	504	0	0	0	0	0	0	0	0	0	0	100
BG	504	0	504	0	0	0	0	0	0	0	0	0	100
CG	504	0	0	504	0	0	0	0	0	0	0	0	100
AB	504	0	0	0	493	0	0	11	0	0	0	0	97.8
AC	504	0	0	0	0	498	0	0	0	6	0	0	98.8
BC	504	0	0	0	0	0	500	0	4	0	0	0	99.2
ABG	504	0	0	0	5	0	0	499	0	0	0	0	99.0
BCG	504	0	0	0	0	0	3	0	501	0	0	0	99.4
ACG	504	0	0	0	0	8	0	0	0	496	0	0	98.4
ABC	504	0	0	0	0	0	0	0	0	0	504	0	100
No fault	10	0	0	0	0	0	0	0	0	0	0	10	100

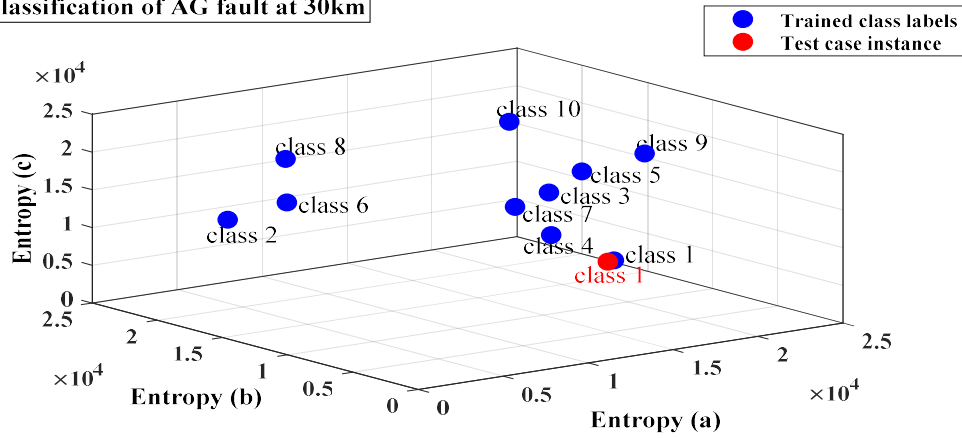
Table 3.7 present the fault events classification accuracy percentage obtained by the DWT and PNN based scheme. However, during the validation of PNN based scheme the case of normal operation is neglected and only fault cases have been considered. It has been observed that the PNN based scheme also provides 100% classification accuracy for LG and LLL fault events. Likewise, the identification accuracy of LL and LLG fault events are 99.53% and 99.07% respectively. The overall average fault events classification accuracy obtained by the proposed PNN classifier based scheme is 99.65%. On the basis of results depicted in Table 3.2, 3.5, and 3.7 it can be concluded that the proposed DWT and non-

parametric ML based scheme is well effective in ascertaining the fault events in the compensated power network with high accuracy percentage. Figure 3.10 (a) to (j) shows the classification of different fault events using the proposed PNN classifier based scheme simulated at 30 km in the test network. The blue dot represents the trained class labels of the fault events; whereas the red dot specifies the output of the classifier model i.e. the particular category of test instance during testing. Figure 3.11 represents the associated confusion matrix obtained during testing. The time for predicting the precise fault events categories in the network by the proposed fault events classification scheme is demonstrated in Table 3.8. The response time is simply the time taken by the trained models for predicting any individual fault event during the testing. By observing Table 3.8, it can be deduced that the developed classifiers models take very less time span for predicting the category of the fault event in the series compensated transmission system.

**Table 3.7** Faults classification accuracy percentage obtained by PNN technique based scheme

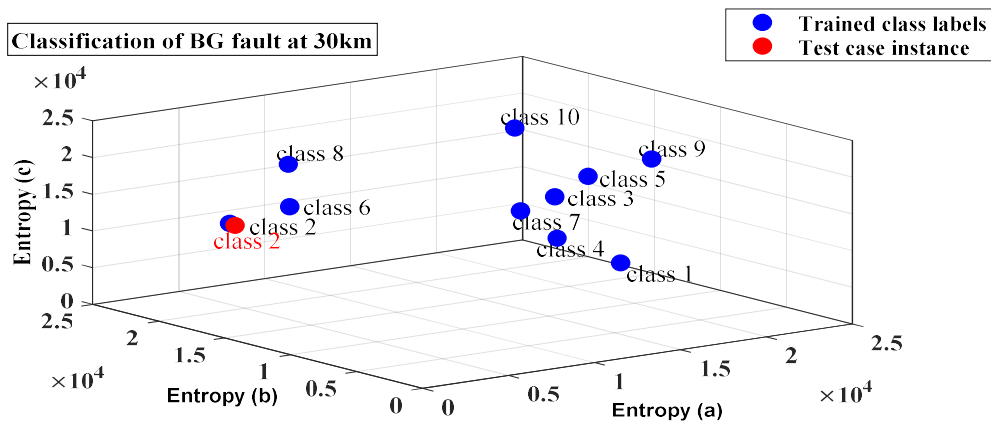
Fault type	Number of test samples	Number of incorrect classification	Correct classification	Over all Accuracy (%)
Line to Ground	1512	0	1512	100.00
Line to Line	1512	7	1505	99.53
Double Line to Ground	1512	14	1498	99.07
3 phase (LLL)	504	0	504	100.00
Avg. Accuracy				99.65

Classification of AG fault at 30km



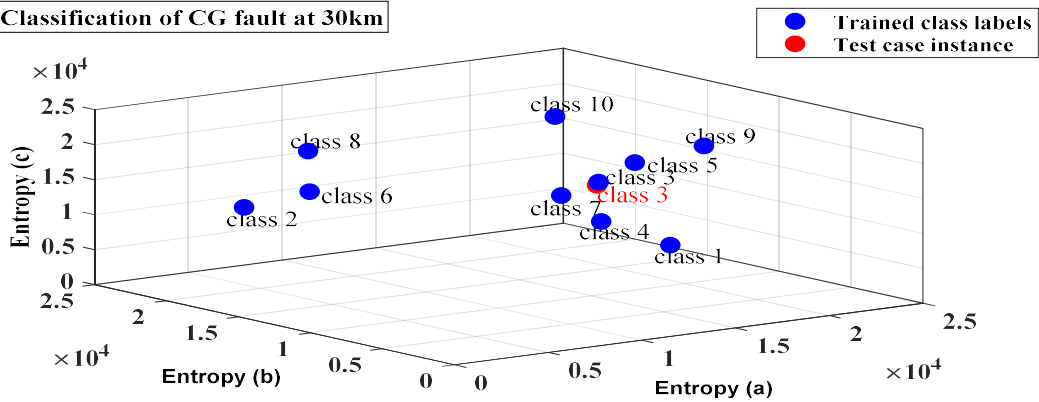
(a)

Classification of BG fault at 30km



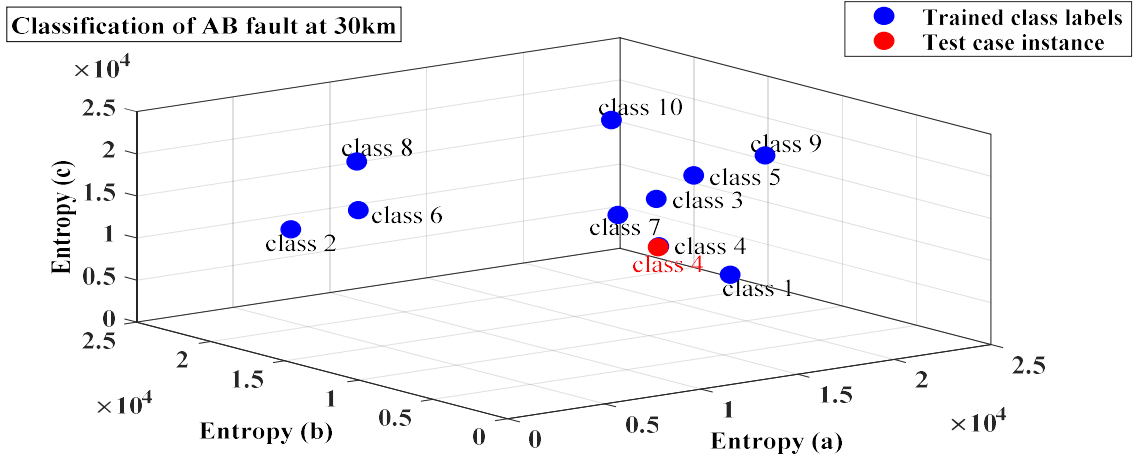
(b)

Classification of CG fault at 30km

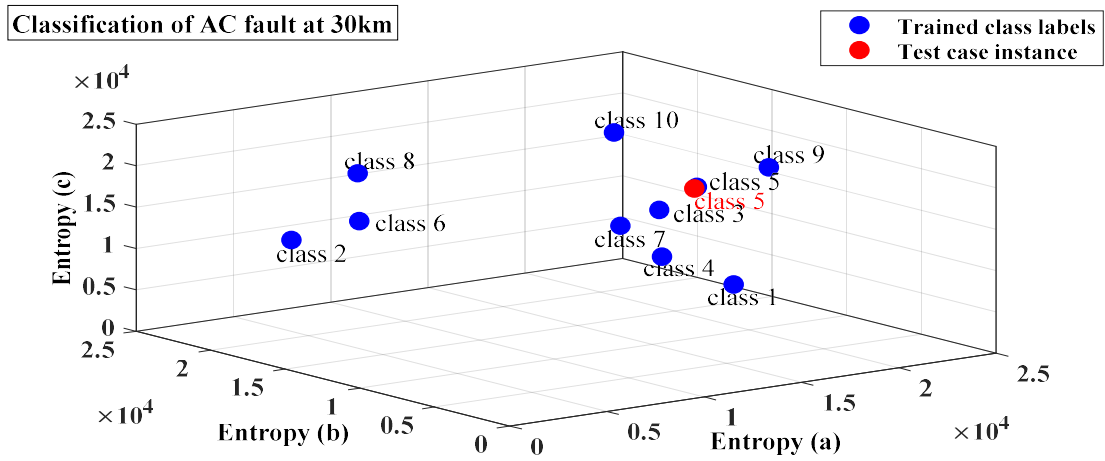


(c)

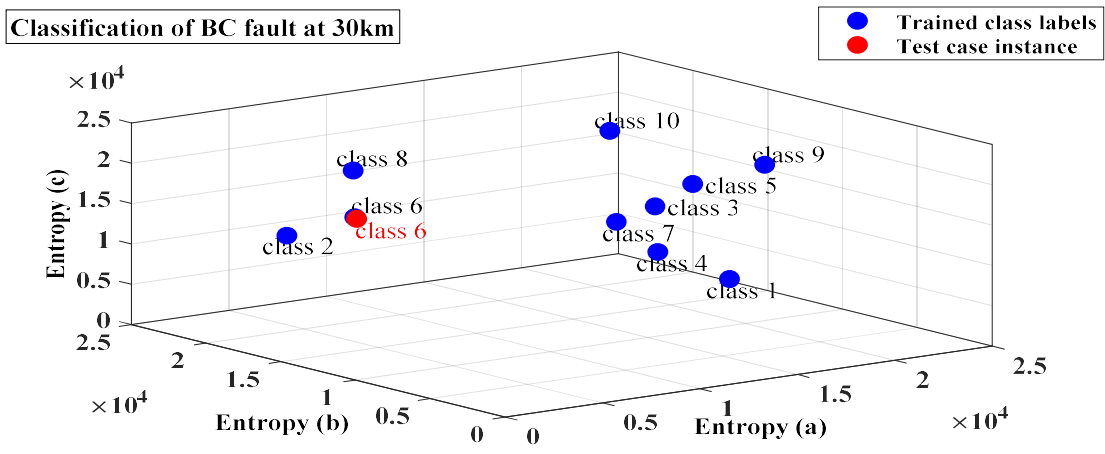




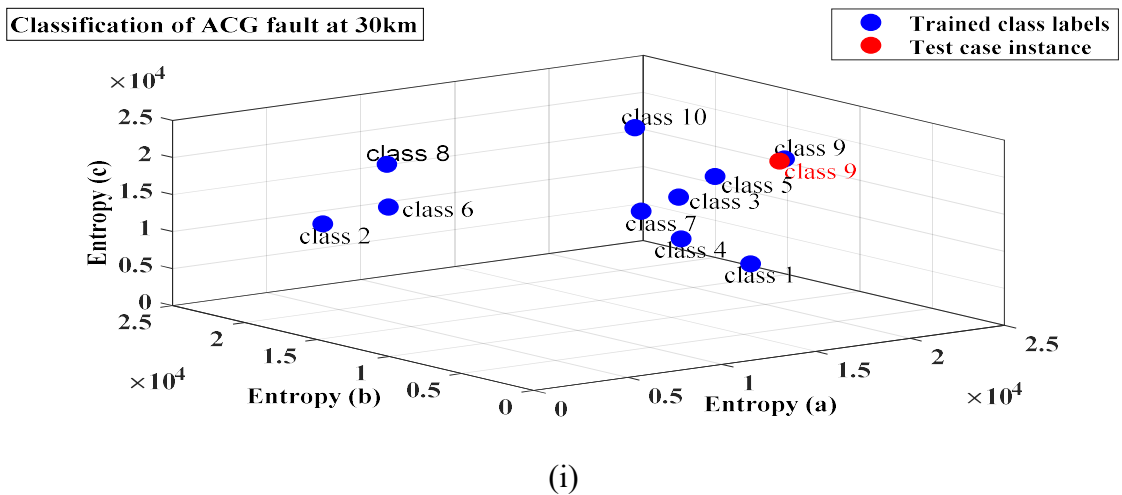
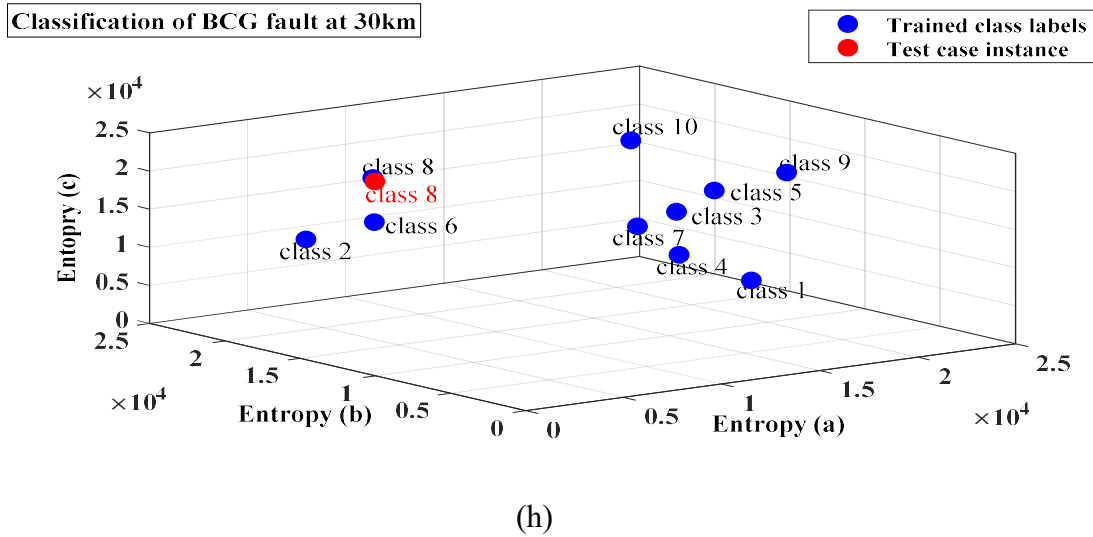
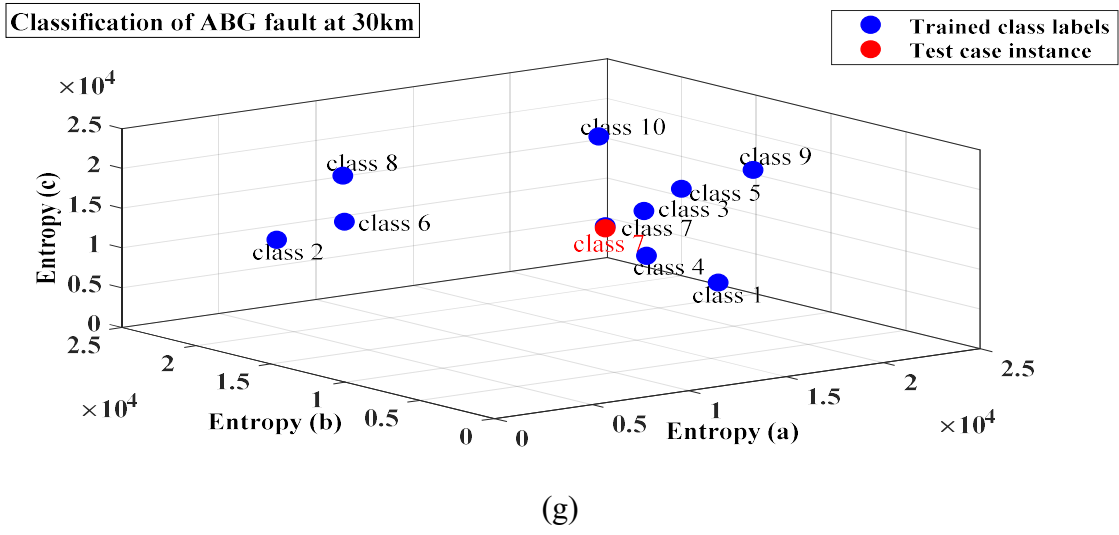
(d)



(e)



(f)



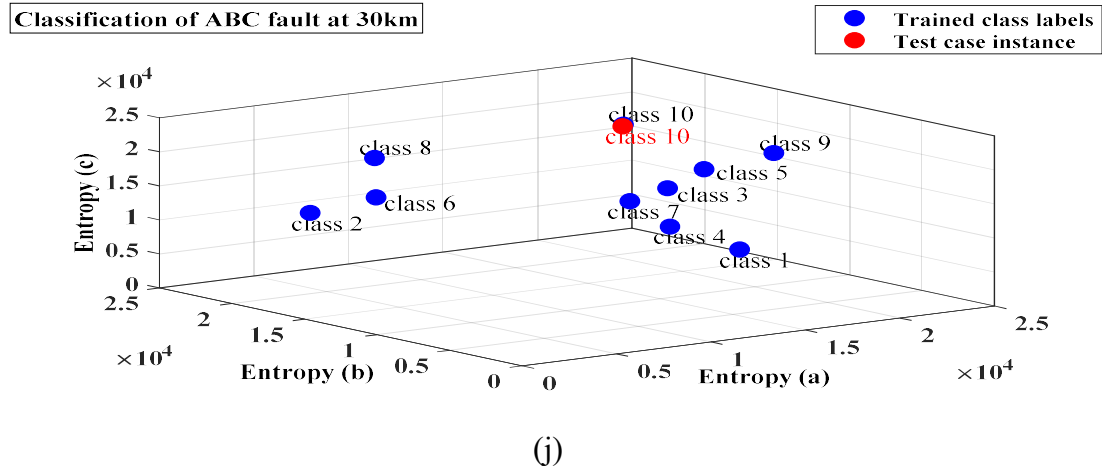


Figure 3.10 Classification of different types of fault events using PNN classifier model (a-j)

		Confusion Matrix (PNN)										
		1	2	3	4	5	6	7	8	9	10	
Output Class	1	504 10.0%	0 0.0%	0 0.0%	0 0.0%	0 0.0%	0 0.0%	0 0.0%	0 0.0%	0 0.0%	0 0.0%	100% 0.0%
	2	0 0.0%	504 10.0%	0 0.0%	0 0.0%	0 0.0%	0 0.0%	0 0.0%	0 0.0%	0 0.0%	0 0.0%	100% 0.0%
	3	0 0.0%	0 0.0%	504 10.0%	0 0.0%	0 0.0%	0 0.0%	0 0.0%	0 0.0%	0 0.0%	0 0.0%	100% 0.0%
	4	0 0.0%	0 0.0%	0 0.0%	501 9.9%	0 0.0%	0 0.0%	5 0.1%	0 0.0%	0 0.0%	0 0.0%	99.0% 1.0%
	5	0 0.0%	0 0.0%	0 0.0%	0 0.0%	500 9.9%	0 0.0%	0 0.0%	0 0.0%	9 0.2%	0 0.0%	98.2% 1.8%
	6	0 0.0%	0 0.0%	0 0.0%	0 0.0%	0 0.0%	504 10.0%	0 0.0%	0 0.0%	0 0.0%	0 0.0%	100% 0.0%
	7	0 0.0%	0 0.0%	0 0.0%	3 0.1%	0 0.0%	0 0.0%	499 9.9%	0 0.0%	0 0.0%	0 0.0%	99.4% 0.6%
	8	0 0.0%	0 0.0%	0 0.0%	0 0.0%	0 0.0%	0 0.0%	0 0.0%	504 10.0%	0 0.0%	0 0.0%	100% 0.0%
	9	0 0.0%	0 0.0%	0 0.0%	0 0.0%	4 0.1%	0 0.0%	0 0.0%	0 0.0%	495 9.8%	0 0.0%	99.2% 0.8%
	10	0 0.0%	0 0.0%	0 0.0%	0 0.0%	0 0.0%	0 0.0%	0 0.0%	0 0.0%	0 0.0%	504 10.0%	100% 0.0%
		100% 0.0%	100% 0.0%	100% 0.0%	99.4% 0.6%	99.2% 0.8%	100% 0.0%	99.0% 1.0%	100% 0.0%	98.2% 1.8%	100% 0.0%	99.6% 0.4%
		1	2	3	4	5	6	7	8	9	10	
		Target Class										

Figure 3. 11 Confusion matrix during events classification using PNN classifier model

Table 3.9 provides the comparative study of the average classification accuracy obtained by the proposed integrated DWT and non-parametric ML based scheme with some already available approaches in the literature [58, 39, 32, and 40]. It has been observed that the proposed DWT and non-parametric ML based scheme provides better fault events classification accuracy and are more competent of handling large feature dataset.

**Table 3.8** Time of response of different non-parametric ML scheme

S. No	Non-Parametric ML Classifier Model Utilized	Time of response
i	K-NN	6.05e-02 s
ii.	SVM	4.14e-02 s
iii.	PNN	1.59e-01 s

**Table 3.9** Comparative study of average classification accuracy achieved by proposed scheme with previously reported approaches

Fault type	Ref. [58] (%)	Ref. [39] (%)	Ref. [32] (%)	Ref. [40] (%)	(SVM) (%)	(KNN) (%)	(PNN) (%)
Line to ground	97.23	97.447	100.00	99.449	100.00	100.00	100.00
Line to line	97.29	99.616	97.560	97.687	98.61	98.809	99.53
Double line to ground	97.84	98.611	98.788	99.314	98.94	99.404	99.07
3 phase (LLL)	97.68	100.00	100.00	98.565	100.00	100.00	100.00
Average accuracy	<b>97.51</b>	<b>98.918</b>	<b>99.087</b>	<b>98.753</b>	<b>99.39</b>	<b>99.553</b>	<b>99.65</b>

### 3.7.2 Test Case-II: Modified IEEE 9-Bus Series Compensated Test Network

The proposed DWT and non-parametric ML based fault events categorization scheme is also validated on the second test system i.e. modified three machines, 9-bus compensated WSCC transmission network (shown in Figure 3.12). The transmission section connecting bus 7 and bus 8 is made 35 % and 45 % compensated by installing the compensating unit close to bus 7. The parameter details of the simulated test WSCC network are provided in the appendix. The details of various considered training and testing conditions on the second test network are listed in Table 3.10. Figure 3.12 represents the 3-phase post fault (A-G) current samples with respect to time (s) at 30 km from the sending side on different fault inception angles. The fault events cases mentioned in Table 3.10 with varying conditions and case of evolving fault events are simulated in the second test system. Later on, the associated extracted feature vectors after the DWT decomposition of the post-fault current samples are applied as input dataset to the non-parametric classifier models during training and testing. The classifier models finally provide the particular class of the test instance on the basis of trained pattern set as its output. The accuracy of fault events classification is computed by equation (3.6).

**Table 3.10** Training and testing conditions considered on second test system

S. No	Parameters	Training cases	Testing cases
1.	Fault locations	Twenty different locations	Five new unknown location (50 km, 110 km, 170 km, 210 km and 250 km)
2.	Fault Resistance (ohms)	0.001, 15, 30	0.1, 1, 5, and 10
3.	Fault inception angle (°)	0, 75, 150	30, 45, 60, 90, and 120
4.	Fault events types	No fault and all	Normal operation mode and

		kinds faults events	all kinds of fault events (unfamiliar)
5.	Level of line compensation	35 % and 45 %	30 % and 40 %

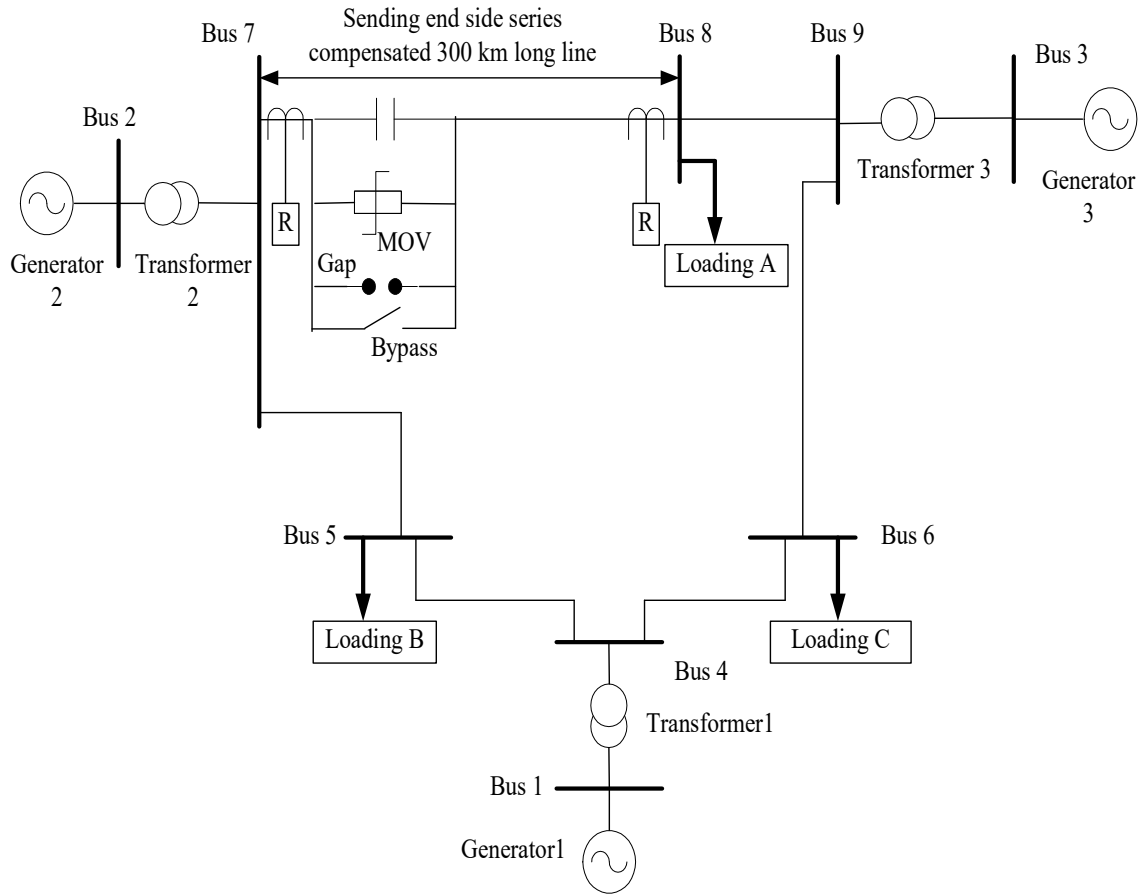
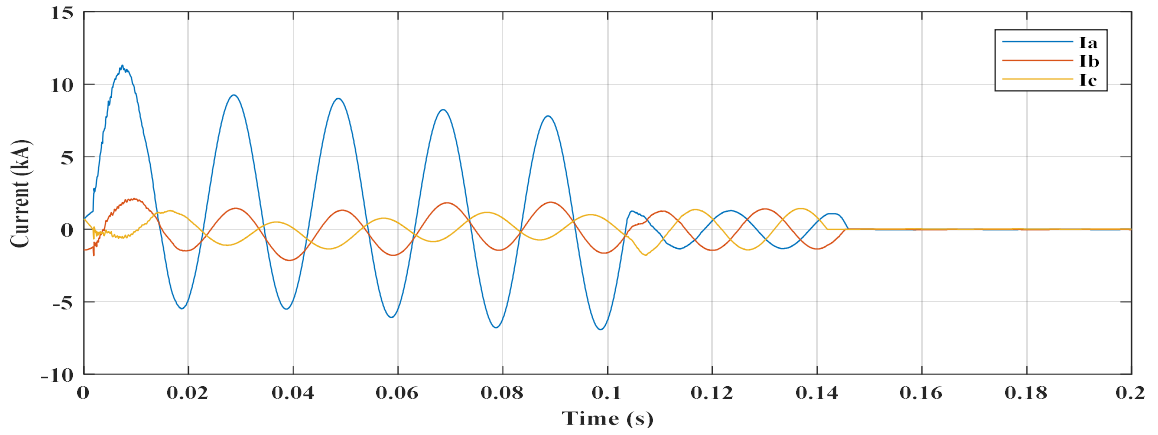
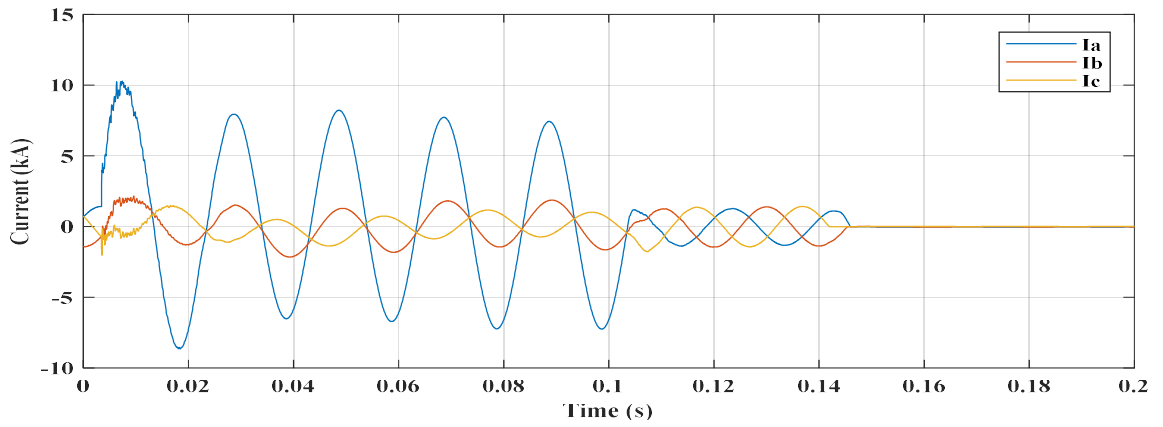


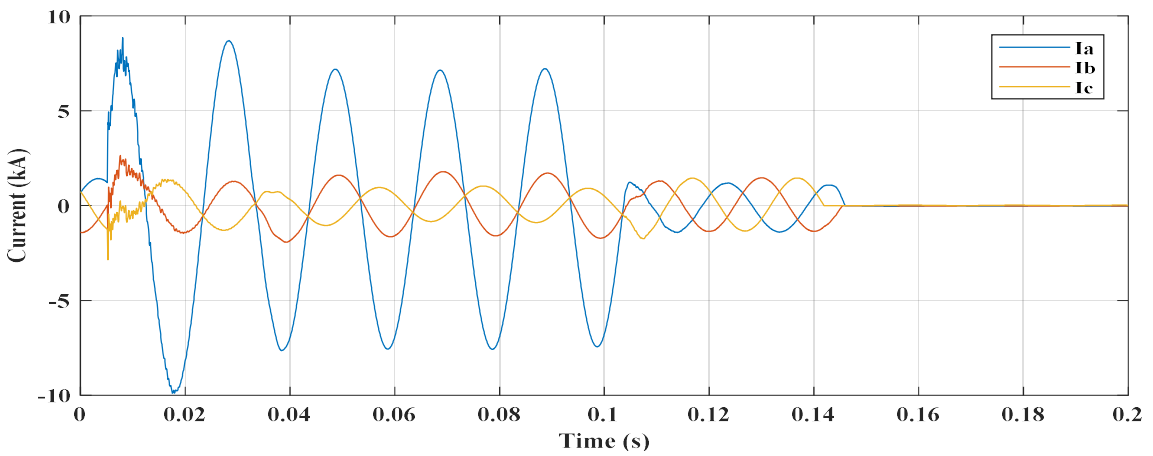
Figure 3.12 Simulated modified WSCC 9-Bus IEEE network (second test system)



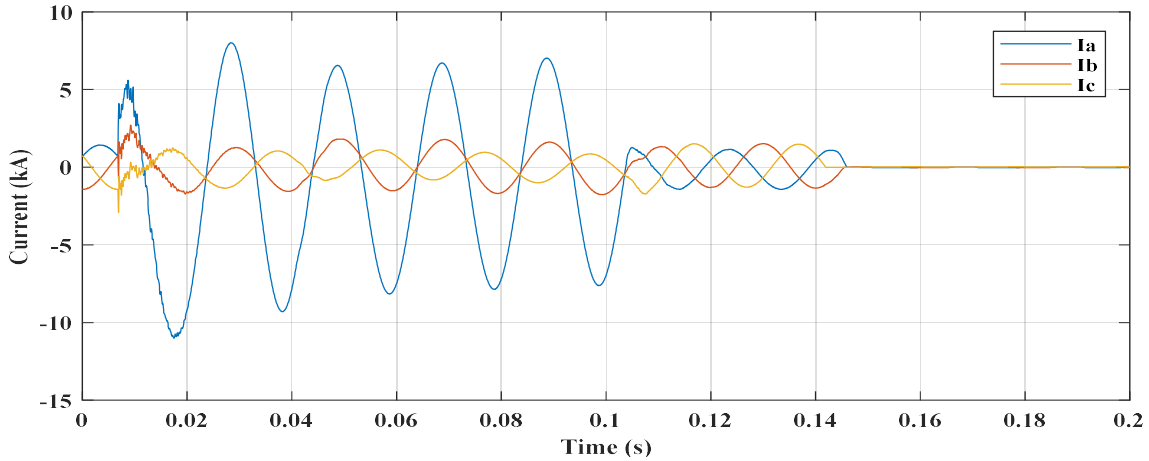
(a)



(b)



(c)



(d)

Figure 3.13 Three phase current signals during line to ground fault event at 50 km on different inception angles (a) 30 degree; (b) 60 degree; (c) 90 degree; (d) 120 degree

Table 3.11 presents the fault events classification accuracy percentage obtained by the proposed DWT and K-NN based scheme during the testing on the second test network. From Table 3.11, it can be observed that proposed K-NN (K=5) based scheme gives 100% classification accuracy for all kinds of fault events in the simulated second test network.

The corresponding confusion matrix for KNN based scheme is shown in Table 3.12.

**Table 3.11** Faults classification accuracy percentage obtained by K-NN technique based scheme

Fault type	Number of test samples	Number of incorrect classification	Correct classification	Over all Accuracy (%)
Line to Ground	600	0	600	100.00
Line to Line	600	0	600	100.00
Double Line to Ground	600	0	600	100.00



3 phase (LLL)	200	0	200	100.00
Avg. Accuracy				100.00

**Table 3.12** Confusion matrix for KNN based scheme (second test system)

Actual fault events	Sample size	Predicted fault events											Accuracy (%)
		AG	BG	CG	AB	AC	BC	ABG	BCG	ACG	ABC	No fault	
AG	200	200	0	0	0	0	0	0	0	0	0	0	100
BG	200	0	200	0	0	0	0	0	0	0	0	0	100
CG	200	0	0	200	0	0	0	0	0	0	0	0	100
AB	200	0	0	0	200	0	0	0	0	0	0	0	100
AC	200	0	0	0	0	200	0	0	0	0	0	0	100
BC	200	0	0	0	0	0	200	0	0	0	0	0	100
ABG	200	0	0	0	0	0	0	200	0	0	0	0	100
BCG	200	0	0	0	0	0	0	0	200	0	0	0	100
ACG	200	0	0	0	0	0	0	0	0	200	0	0	100
ABC	200	0	0	0	0	0	0	0	0	0	200	0	100
No fault	10	0	0	0	0	0	0	0	0	0	0	10	100

**Table 3.13** Faults classification accuracy percentage obtained by SVM technique based scheme

Fault type	Number of test samples	Number of incorrect classification	Correct classification	Over all Accuracy (%)
Line to Ground	600	0	600	100.00
Line to Line	600	12	588	98.00
Double Line to Ground	600	8	592	98.67
3 phase (LLL)	200	0	200	100.00
Avg. Accuracy				99.17

Table 3.13 shows the results in terms of classification accuracy obtained by the proposed DWT and SVM based scheme during testing on second test system. The overall average fault events classification accuracy obtained on the second test network by the proposed SVM classifier model based scheme is 99.17%. The corresponding confusion matrix for SVM based scheme is shown in Table 3.14.

**Table 3.14** Confusion matrix for SVM based scheme (Second test system)

Actual fault events	Sample size	Predicted fault events											Accuracy (%)
		AG	BG	CG	AB	AC	BC	ABG	BCG	ACG	ABC	No fault	
AG	200	200	0	0	0	0	0	0	0	0	0	0	100
BG	200	0	200	0	0	0	0	0	0	0	0	0	100
CG	200	0	0	200	0	0	0	0	0	0	0	0	100
AB	200	0	0	0	194	0	0	6	0	0	0	0	97.0

AC	200	0	0	0	0	196	0	0	0	4	0	0	98.0
BC	200	0	0	0	0	0	198	0	2	0	0	0	99.0
ABG	200	0	0	0	3	0	0	197	0	0	0	0	98.5
BCG	200	0	0	0	0	0	0	0	200	0	0	0	100
ACG	200	0	0	0	0	5	0	0	0	194	0	0	97.0
ABC	200	0	0	0	0	0	0	0	0	0	200	0	100
No fault	10	0	0	0	0	0	0	0	0	0	0	10	100

**Table 3.15** Faults classification accuracy percentage obtained by PNN technique based scheme

Fault type	Number of test samples	Number of incorrect classification	Correct classification	Over all Accuracy (%)
Line to Ground	600	0	600	100.00
Line to Line	600	0	600	100.00
Double Line to Ground	600	4	596	99.33
3 phase (LLL)	200	0	200	100.00
Avg. Accuracy				99.83

Table 3.15 provides the fault events classification accuracy percentage acquired by the proposed DWT and PNN based scheme during testing on the second test network. It can be observed that proposed PNN based scheme gives 100% classification accuracy for LG, LL, and LLL fault events. The overall average fault events classification accuracy obtained by the proposed PNN classifier model based scheme is 99.83%. The Figure 3.14 shows the corresponding confusion matrix obtained during testing of PNN based scheme on second simulated test network.

		Confusion Matrix (PNN)										
Output Class		Target Class										
		1	2	3	4	5	6	7	8	9	10	
1	200 10.0%	0 0.0%	0 0.0%	0 0.0%	0 0.0%	0 0.0%	0 0.0%	0 0.0%	0 0.0%	0 0.0%	0 0.0%	100% 0.0%
2	0 0.0%	200 10.0%	0 0.0%	0 0.0%	0 0.0%	0 0.0%	0 0.0%	0 0.0%	0 0.0%	0 0.0%	0 0.0%	100% 0.0%
3	0 0.0%	0 0.0%	200 10.0%	0 0.0%	0 0.0%	0 0.0%	0 0.0%	0 0.0%	0 0.0%	0 0.0%	0 0.0%	100% 0.0%
4	0 0.0%	0 0.0%	0 0.0%	200 10.0%	0 0.0%	0 0.0%	0 0.0%	0 0.0%	0 0.0%	0 0.0%	0 0.0%	100% 0.0%
5	0 0.0%	0 0.0%	0 0.0%	0 0.0%	200 10.0%	0 0.0%	0 0.0%	0 0.0%	4 0.2%	0 0.0%	98.0% 2.0%	
6	0 0.0%	0 0.0%	0 0.0%	0 0.0%	0 0.0%	200 10.0%	0 0.0%	0 0.0%	0 0.0%	0 0.0%	100% 0.0%	
7	0 0.0%	0 0.0%	0 0.0%	0 0.0%	0 0.0%	0 0.0%	200 10.0%	0 0.0%	0 0.0%	0 0.0%	100% 0.0%	
8	0 0.0%	0 0.0%	0 0.0%	0 0.0%	0 0.0%	0 0.0%	0 0.0%	200 10.0%	0 0.0%	0 0.0%	100% 0.0%	
9	0 0.0%	0 0.0%	0 0.0%	0 0.0%	0 0.0%	0 0.0%	0 0.0%	0 0.0%	196 9.8%	0 0.0%	100% 0.0%	
10	0 0.0%	0 0.0%	0 0.0%	0 0.0%	0 0.0%	0 0.0%	0 0.0%	0 0.0%	0 0.0%	200 10.0%	100% 0.0%	
		100% 0.0%	100% 0.0%	100% 0.0%	100% 0.0%	100% 0.0%	100% 0.0%	100% 0.0%	98.0% 2.0%	100% 0.0%	99.8% 0.2%	

Figure 3. 14 Confusion matrix during events classification using PNN classifier model

### 3.8 Evolving Fault Events Identification

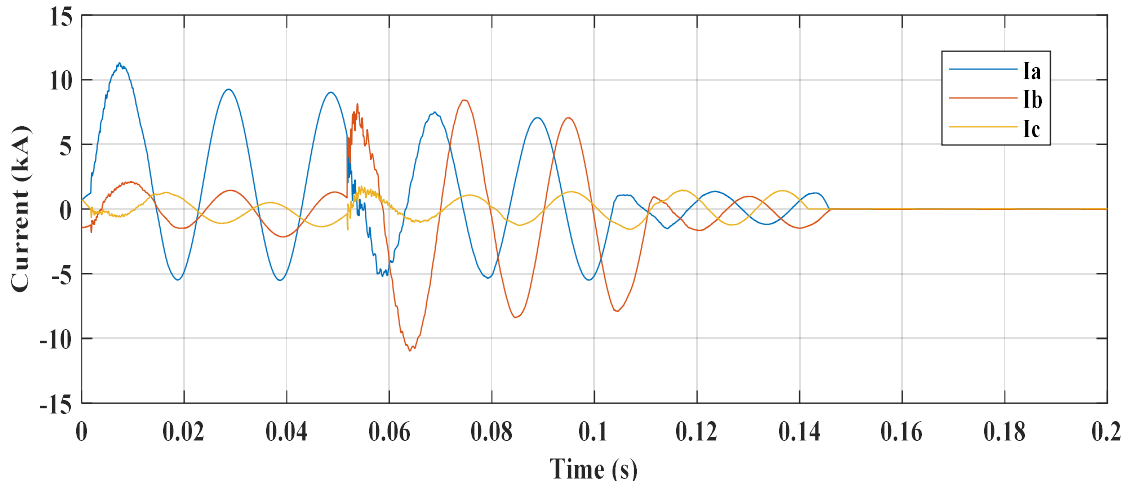
Evolving fault events (EFE) are the faults in the transmission network which are actuated in one phase and subsequently within few cycles involve other phases also. Evolving events in the transmission network are much more complicated than the commonly occurring shunt fault events mainly because of transition of phases are involved in it. The shifting of

involved phases during evolving events with respect to time span makes the faulty phase recognition mechanism more complicated for the relaying system. In evolving abnormality cases, the initial fault is usually called as the primary fault and the subsequent event is termed as the secondary fault. Figure 3.15 shows the 3-phase fault current samples during the case of evolving fault event actuated in the simulated transmission circuit at 50 km from the bus 7 in the second test network. The evolving events started with the first phase i.e. primary abnormality A-G fault at 0.00166 seconds and expanded to another phase subsequently i.e. secondary abnormality B-G after 5ms. In present work, three different times interval i.e. 5 milliseconds, 10 milliseconds, and 15 milliseconds between primary and secondary fault events have been considered. Similarly, two other evolving events i.e. AG-CG and AG-ABCG are shown in the Figure 3.15 (b), (c) below. The details of different evolving fault events considered during the training and testing of the proposed DWT and non-parametric ML based scheme are listed in Table 3.16. The test sample consists of four normal shunt events, three types of evolving events with varying conditions such as locations in the network, fault resistances, inception angles, and line compensation percentage levels. Hence, the total size of the testing samples is 4200 (four types of normal shunt events, three types of evolving events, four different set of fault resistances, five inception angles, two level of line compensation percentage and three different time interval between initial and secondary fault events). The post-fault current samples retrieved during usual shunt fault and evolving fault events are decomposed by DWT mechanism for computing the dominant fault feature vectors. The associated extracted feature vectors for both normal shunt fault and evolving fault events are applied as input dataset to the non-parametric classifier models during training and testing. The different

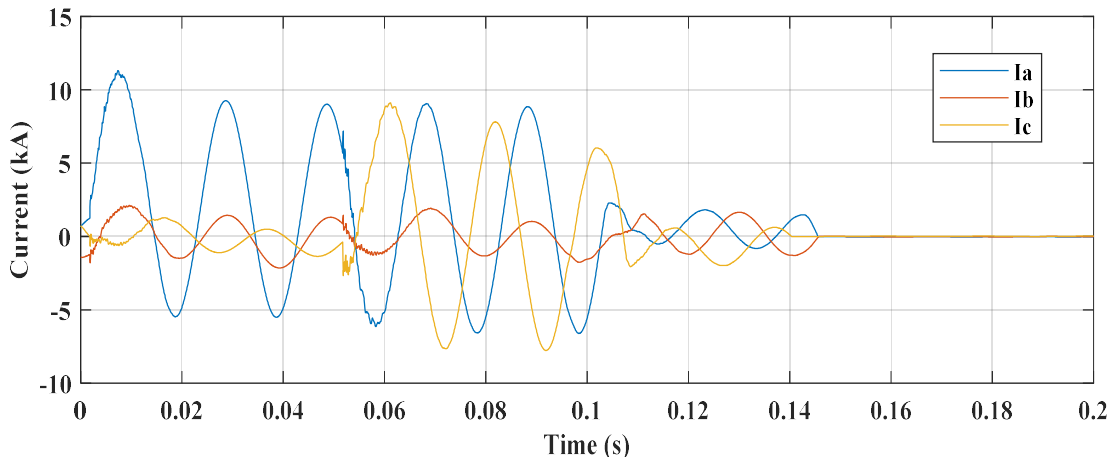
fault events as labelled as follows: Class 1 (AG), class 2 (ABG), class 3 (AB-bg), class 4 (ACG), class 5 (AG-cg), class 6 (ABC), class 7 (AG-abcg). Finally, the ML classifier models discriminate the normal and evolving fault events into their specific class labels as its output.

**Table 3.16** Training and testing conditions for assessing evolving fault events

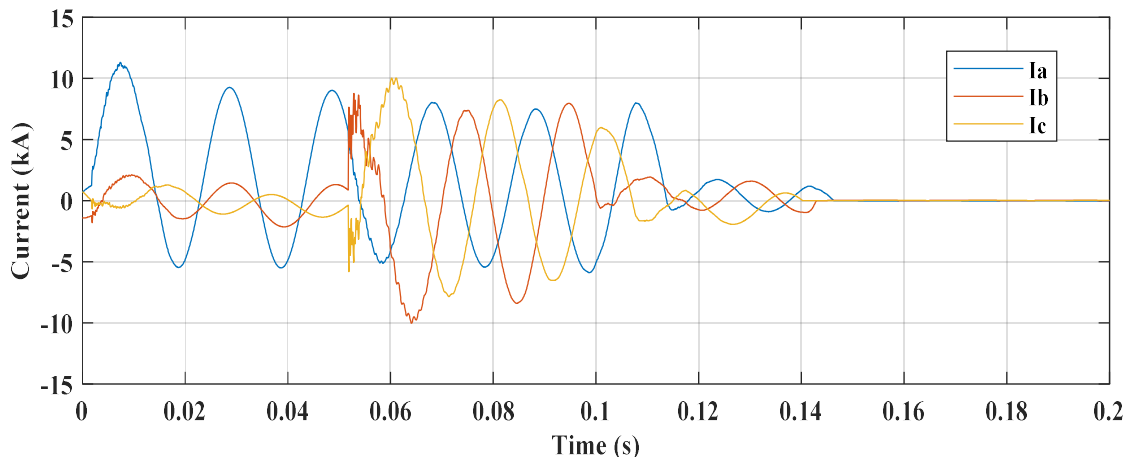
S. No	Parameters	Training cases	Testing cases
1.	Fault locations (km)	Twenty different locations	Five new unknown location (50km, 110 km, 170 km, 210 km and 250 km)
2.	Fault Resistance (ohms)	0.001, 15, 30	0.1, 1, 5, and 10
3.	Fault inception angle (°)	0, 75, 150	30, 45, 60, 90, and 120
4.	Fault events types	AG, ABG, ACG, ABC, AG-bg, AG-cg and AG-abcg	AG, ABG, ACG, ABC, AG-bg, AG-cg and AG-abcg
5.	Level of line compensation	35 % and 45 %	30 % and 40 %
6.	Time delay		5, 10, and 15 ms



(a)



(b)



(c)

Figure: 3. 15 3-phase current samples during evolving fault in the test network  
 (a) AG-bg at 50 km, (b) AG-cg at 50 km, (c) AG-abcg at 50 km

Table 3.17 presents the evolving faults classification results obtained by the proposed DWT and K-NN based scheme. Similarly, Table 3.18 provides the evolving faults classification results obtained by the proposed DWT and SVM based scheme. From both Tables 3.17 and 3.18 it can be observed that proposed K-NN and SVM based schemes are well effectual in discriminating the normal shunt faults and evolving fault events.

**Table 3.17** Identification of evolving fault events using KNN classifier based scheme

S.No	Primary fault type	Secondary fault type	Time interval (ms)	Evolving Fault or not	Classifier output
1.	AG	-	-	No	1
2.	ABG	-	-	No	2
3.	AG	bg	5	Yes	3
4.	ACG	-	-	No	4
5.	AG	cg	5	Yes	5
6.	ABC	-	-	No	6
7.	AG	abcg	5	Yes	7
8.	AG	bg	10	Yes	3
9.	AG	cg	10	Yes	5
10.	AG	abcg	10	Yes	7
11.	AG	bg	15	Yes	3
12.	AG	cg	15	Yes	5
13.	AG	abcg	15	Yes	7

**Table 3.18** Identification of evolving fault events using SVM classifier based scheme

S.No	Primary fault type	Secondary fault type	Time interval (ms)	Evolving Fault or not	Classifier output
1.	AG	-	-	No	1
2.	ABG	-	-	No	2
3.	AG	bg	5	Yes	3
4.	ACG	-	-	No	4
5.	AG	cg	5	Yes	5



6.	ABC	-	-	No	6
7.	AG	abcg	5	Yes	7
8.	AG	bg	10	Yes	3
9.	AG	cg	10	Yes	5
10.	AG	abcg	10	Yes	7
11.	AG	bg	15	Yes	3
12.	AG	cg	15	Yes	5
13.	AG	abcg	15	Yes	7

Table 3.19 shows the evolving fault classification results obtained by the proposed DWT and PNN based scheme. It has been observed that the PNN based scheme is also well competent in identifying the evolving fault events in the compensated power network with 100% classification accuracy. The Figure 3.16 shows the corresponding confusion matrix obtained during the testing.

**Table 3.19** Evolving fault events classification percentage obtained by PNN based scheme

Fault type	Number of test samples	Number of incorrect classification	Correct classification	Over all Accuracy (%)
AG	600	0	600	100
ABG	600	0	600	100
AG-bg (evolving event)	600	0	600	100
ACG	600	0	600	100
AG-cg (evolving event)	600	0	600	100
ABC	600	0	600	100
AG-abcg (evolving event)	600	0	600	100

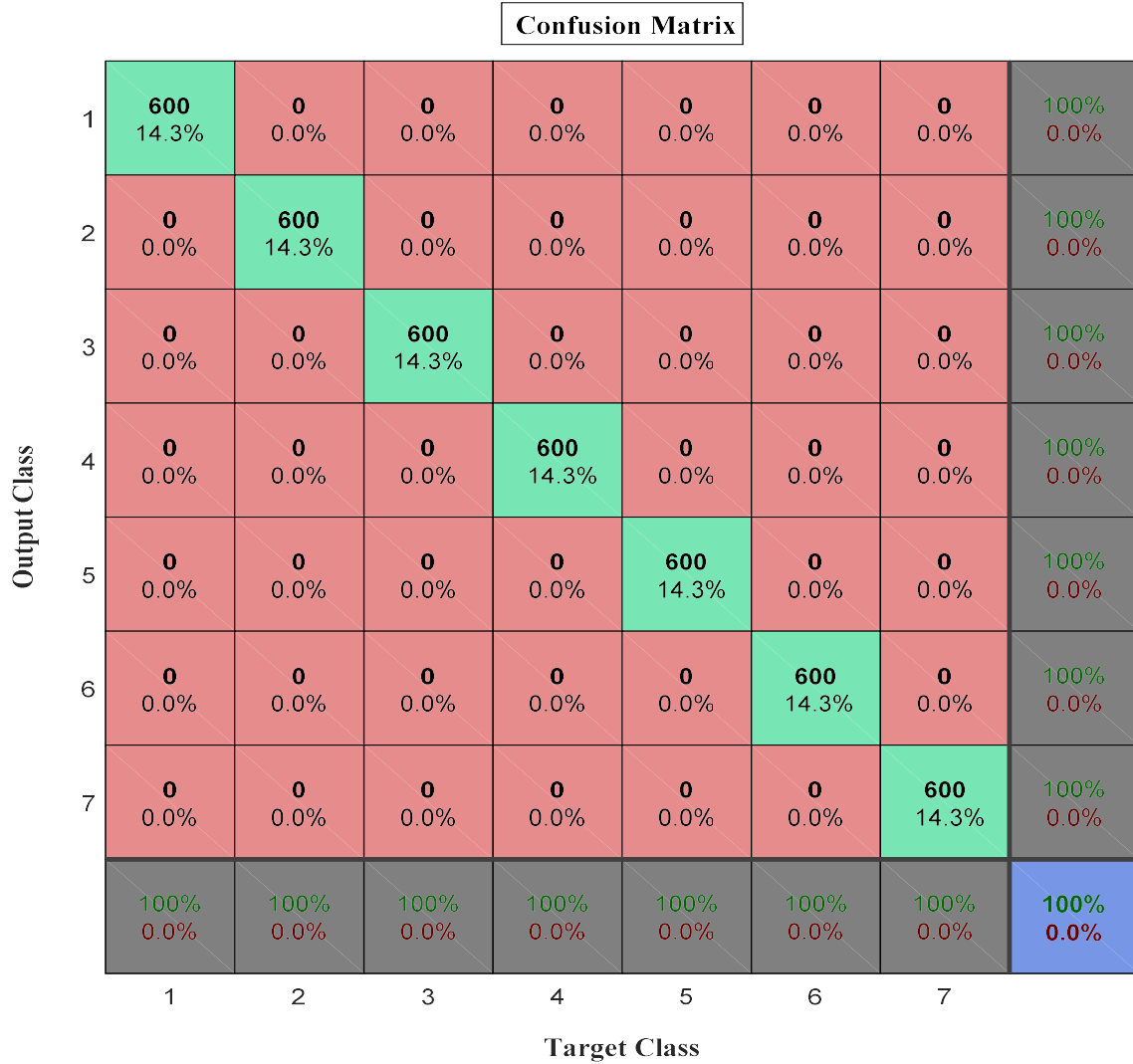
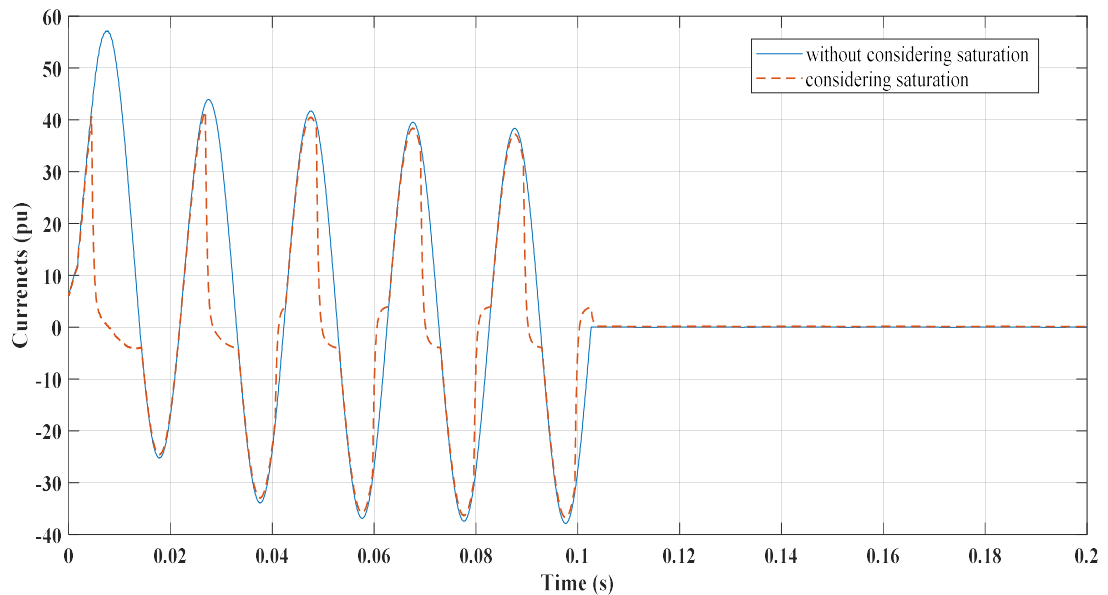
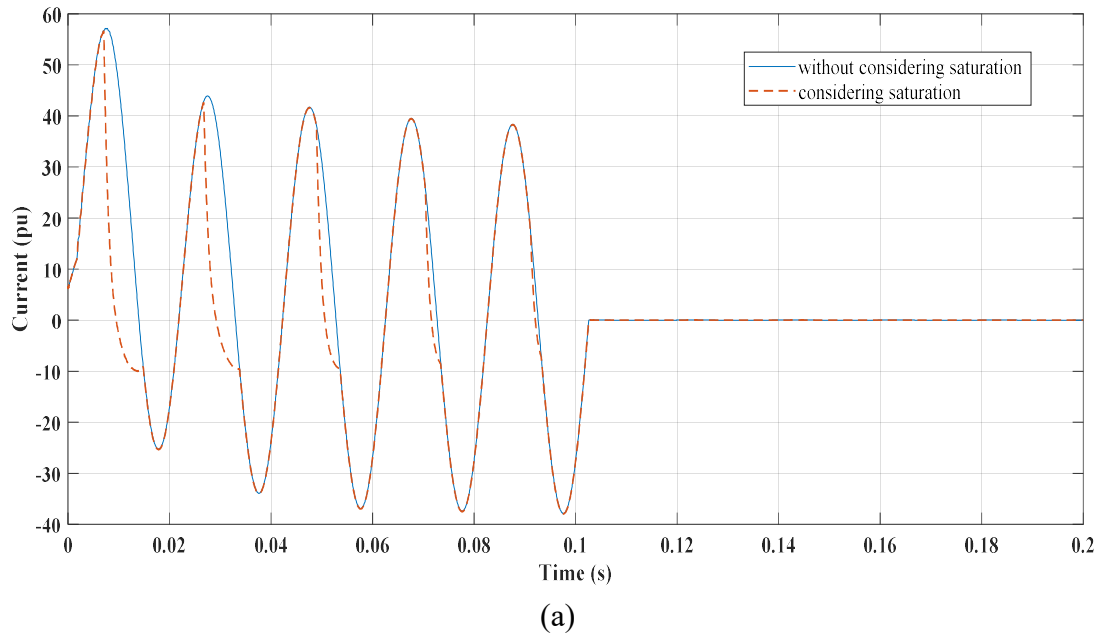


Figure 3.16 Confusion matrix during classification of evolving fault events

### 3.9 Performance During CTs Saturation

The saturation phenomena of CTs are almost inevitable in the transmission network because of incorporation of power electronic devices and large current values during abnormalities in the network. It can be one of the major causes of malfunctioning of lineal relaying system. The consideration of CTs saturation is not very common in available reported protection schemes for series compensated power network. In the present study the effect of CTs saturation on the performance of proposed approach has been significantly

investigated. The efficacy of the proposed scheme has been examined during the condition of CTs saturation for various test cases on three different burden resistances (2ohm, 5ohm and 10 ohm). Figure 3.17 shows the fault (AG) current signals in a 40 % compensated power network with and without considering CTs saturation at 30 km from the sending terminals with varying conditions.



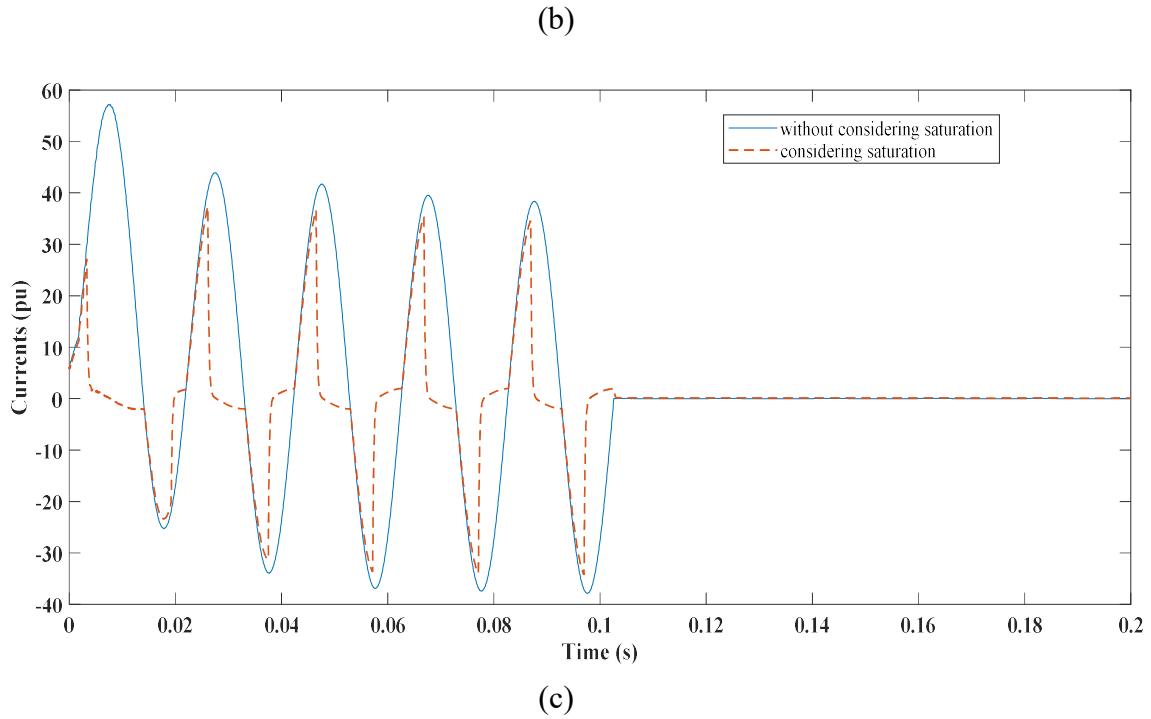


Figure 3.17 Fault current signals at 40 % line compensation with and without considering CTs saturation((a) A-G at 30 km, with FIA 30 degree, FR 0.1 ohm, CT burden 2 ohm; (b) A-G at A-G at 30 km, with FIA 30 degree, FR 0.1 ohm, CT burden 5 ohm; (c) A-G at 50 km, A-G at 30 km, with FIA 30 degree, FR 0.1 ohm, CT burden 10 ohm)

It has been noticed that the competency of proposed events categorization scheme remains unaffected irrespective of CTs saturation at different burden levels. The simulation results during the saturation are presented in Table 3.20. However, the overall fault events classification accuracy acquired during the CTs saturation condition is comparatively less than during without considering the saturation phenomena.

**Table 3.20** Performance of proposed classifier models during saturation at three different burden impedances

Simulated test parameters	Actual fault type	KNN output	PNN output
Five unknown fault locations with varying fault resistance, inception angle and level of line compensation	No fault	No fault	No fault
	LG event	LG	LG
	LLG	LLG	LLG
	LL	LL	LL
	LLL	LLL	LLL

### 3.10 Conclusion

The primary layout of the proposed integrated DWT and ML based scheme for ascertaining the fault events in the compensated power transmission network is presented in this chapter. The fundamentals of machine learning techniques utilized in this work have been thoroughly described. Then the work-flow, training and testing mechanism of the proposed events classification scheme are explained. Further, the feasibility and competency of the proposed integrated DWT and non-parametric ML based fault events ascertaining scheme is analyzed for various shunt fault scenarios on two distinct simulated test networks. In addition, the performance of the proposed scheme is also evaluated for transforming fault events and during CTs saturation condition. By seeing the obtained results for varying fault scenarios, it has been reaffirmed that the proposed scheme is well competent in ascertaining

the fault events in series compensated power network irrespective of varying fault conditions.